1-1-2005

Field Monitoring Prototype Retrofits of Floorbeam Connections on the I-95 Girard Point Bridge

Hassam N. Mahmoud

Robert J. Connor

Field Monitoring Prototype Retrofits of Floorbeam Connections on the I-95 Girard Point Bridge

Final Report

by

Hussam N. Mahmoud

Robert J. Connor

ATLSS Report No. 05-01

January 2005

ATLSS is a National Center for Engineering Research on Advanced Technology for Large Structural Systems

117 ATLSS Drive
Bethlehem, PA 18015-4729

Phone: (610)758-3525
Fax: (610)758-5902

www.atlss.lehigh.edu
Email: inatl@lehigh.edu

Field Monitoring Prototype Retrofits of Floorbeam Connections on the I-95 Girard Point Bridge

Final Report

by

Hussam N. Mahmoud
Research Engineer
ATLSS Engineering Research Center

Robert J. Connor
Research Engineer
ATLSS Engineering Research Center

ATLSS Report No. 05-01

January 2005

ATLSS is a National Center for Engineering Research on Advanced Technology for Large Structural Systems

117 ATLSS Drive
Bethlehem, PA 18015-4729

Phone: (610)758-3525
Fax: (610)758-5902

www.atlss.lehigh.edu
Email: inatl@lehigh.edu

Table of Contents

		Page
EXECUTIVE SUMMARY		**1**
1.0	**Introduction and Background**	**2**
	1.1 Bridge Description	2
2.0	**Instrumentation Plan and Data Acquisition**	**3**
	2.1 Strain Gages	3
	2.2 Displacement Sensors	4
	2.3 Data Acquisition	4
	2.4 Uncontrolled Monitoring	5
3.0	**Controlled Load Testing**	**6**
4.0	**Summary of Instrumentation Layout**	**9**
	4.1 Prototype retrofits	9
	4.2 Initial Retrofit – FB77	10
	4.2.1 Strain Gages on the Web of the Floorbeam around the Cutout	10
	4.2.2 Strain Gages on Floorbeam Web below the Cutout at Longitudinal Stiffener Termination	10
	4.2.3 Gage on the Web at Transverse Stiffener Detail	11
	4.2.4 Gage on the Web at Longitudinal Stiffener to Transverse Stiffener Detail	12
	4.2.5 Gages on Top and Bottom Flanges of the Floorbeam	12
	4.2.6 Gages on Top and Bottom Flanges of the Stringer	13
	4.2.7 Displacement Sensors	14
	4.3 Initial Retrofit with Rivets Removed – FB77	14
	4.4 Modified Retrofit – FB78	15
	4.4.1 Strain Gages on the Web of the Floorbeam around and below the Cutout	15
	4.4.2 Strain Gages on the Web of the Floorbeam and the Angle Attaching the Floorbeam to the Truss Hanger	16
5.0	**Results of Controlled Load Tests**	**18**
	5.1 Crawl Test	18
	5.1.1 Stresses on the Floorbeam Web around the Cutout	18
	5.1.2 Stresses at Floorbeam Web below the Cutout at Longitudinal Stiffener Termination	20
	5.1.3 Stresses at the Web of the Floorbeam at Transverse Stiffener Detail	21
	5.1.4 Stresses at Floorbeam Web below the Cutout at Longitudinal Stiffener Termination	22
	5.1.5 Stresses at the Web at Longitudinal Stiffener to Transverse Stiffener Detail	24

Page

5.1.6 Stresses at Top and Bottom Flanges of the Floorbeam 25
5.1.7 Stresses at Top and Bottom Flanges of the Stringer 27
5.2 Dynamic Tests 29
5.2.1 Stresses on the Floorbeam Web around the Cutout 30
5.2.2 Stresses at Floorbeam Web below the Cutout at Longitudinal Stiffener Termination 32
5.2.3 Stresses at the Web of the Floorbeam at Transverse Stiffener Detail 33
5.2.4 Stresses at Floorbeam Web below the Cutout at Longitudinal Stiffener Termination 33
5.2.5 Stresses at the Web at Longitudinal Stiffener to Transverse Stiffener Detail 34
5.2.6 Stresses at Top and Bottom Flanges of the Floorbeam 34
5.2.7 Stresses at Top and Bottom Flanges of the Stringer 36

6.0 Long-Term Monitoring 37
6.1 Results of Long-Term Monitoring 37
6.1.1 Stresses in the Web of Floorbeam FB77 around the Cutout – Initial Retrofit 37
6.1.2 Stresses in the Web of Floorbeam FB77 around the Cutout – Initial Retrofit with Rivets Removed 39
6.1.3 Stresses in the Web of Floorbeam FB78 around the Cutout – Second Retrofit 40

7.0 Summary and Conclusions 42

References 43

APPENDIX A – Instrumentation Plans

EXECUTIVE SUMMARY

Cracking problems at various locations on the Girard Point Bridge have been reported since 1993. In this study the cracks under investigation existed in the floorbeam-to-kneebrace connection in the main span. A poor quality flame cut radius hole (at the termination of the top flange of the floorbeam) and poor quality workmanship introduced both gouges and other crack initiators [1]. The cracks initiated and were driven by the relative displacement between the top flange of the floorbeam and the associated vertical hanger of the truss. To eliminate the problem, two prototype retrofits were proposed by the firm of URS and implemented at floorbeam FB77 and FB78. The rational behind both retrofits was to soften the detail by removing a portion of the web and flange of the floorbeam in order to provide sufficient flexibility to allow for the movement between the top flange of the floorbeam and the hanger. Both details were instrumented to quantify the applicability of both prototype retrofits and to estimate their remaining fatigue life.

Field testing of the first retrofit was conducted to characterize the response of floorbeam FB77 to moving loads with known weight. Two test trucks (72,800 lb and 68,920 lb) were used in both the crawl and dynamic tests. Specifically, one crawl test was conducted using both test trucks (side-by-side) and six dynamic tests were conducted using a single test truck. In addition to controlled load testing, remote monitoring was also conducted for a period of 11 days. The data were collected as random vehicles crossed the bridge. Field testing and remote monitoring of the first prototype retrofit showed that high stress-range cycles existed on the web of the floorbeam near the edge of the cutout. Although fatigue life calculations suggested that the remaining life of the instrumented details was infinite at most locations, high stress range cycles approaching the CAFL of the detail were measured.

In order to reduce the magnitude of the stress range experienced by the details in the floorbeam FB77 and redirect the stress flow downward and away from the area of the web cut near the connection angles, eighteen rivets used in the angle connection between the floorbeam web to the truss hanger were removed. The retrofitted floorbeam FB77 with the rivets removed was monitored for 6.75 days. Removing the rivets was slightly effective in reducing the magnitude of the stresses around the cutout near the connection angle. Also, details where finite life was estimated, no improvement in life was observed. Hence, it was felt that the reduction was not sufficient enough such that the retrofit could be implemented on the remainder of the floorbeams on the bridge. As a result of the above mentioned a second retrofit was proposed by the firm of URS and implemented at floorbeam FB78. Remote monitoring of the prototype retrofit was conducted for a period of 1.4 days. This second retrofit was successful in significantly reducing the maximum measured stresses in the web of the cutout.

1.0 Introduction and Background

1.1 Bridge Description

The Girard Point Bridge was built in 1985 and carries Interstate 95 over the Schuylkill River. The bridge is a three-span cantilever-suspended truss with a 700 ft main span and two side spans of 350 ft. Simple span deck trusses of 200 and 300 feet in length also exist on each approach. The bridge has two decks (upper and lower), with three south bound lanes on the upper deck and three north bound lanes on the lower deck. A retrofit to the pin and hanger connections supporting the center suspended span was completed in 1995 by installing four high strength stainless steel rods at the four hangers. Figure 1.1 shows an elevation view of the Girard Point Bridge looking west.

Figure 1.1 – Side view of the Girard Point Bridge over the Schuylkill River
(Courtesy of Modjeski and Masters)

The bridge has experienced cracking problems at various locations since 1993 [1]. The cracking under investigation in this study exists at the floorbeam-to-kneebrace connections (Figure 1.2). The cracks originated at the flame cut radius hole where the top flange is terminated as well as along the web-to-flange weld in the floorbeam. The initiation of the cracks was driven by the relative displacement between the top flange of the floorbeam and the hanger of the bridge. At several locations, cracks branched and propagated in the direction perpendicular to the primary bending stresses in the floorbeam. Detailed listings of the location of the cracks could be found in the inspection report prepared by the firm of URS Corporation [1].

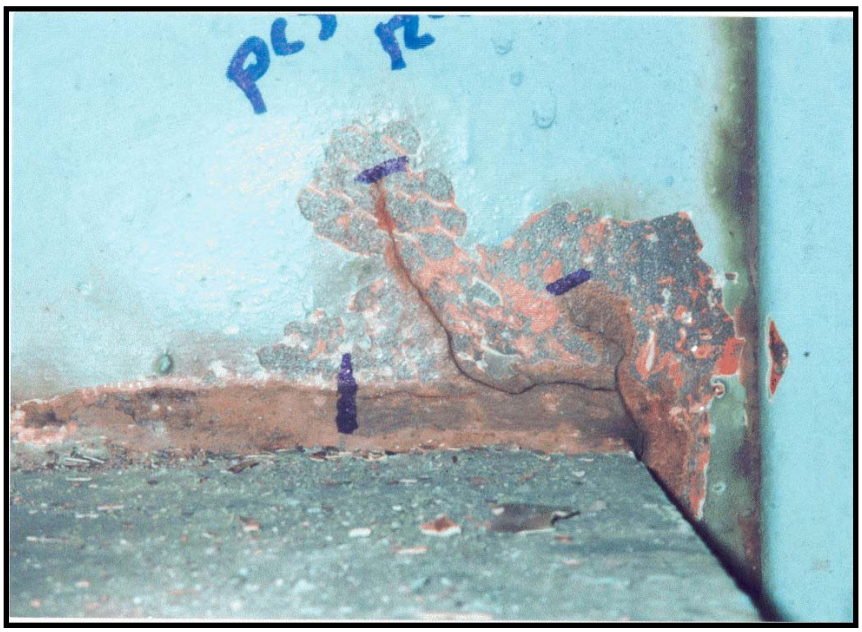

Figure 1.2 – Typical cracking of floorbeam-to-kneebrace connection

With the aid of ATLSS researchers, the firm of URS developed and proposed a retrofit strategy to repair the cracked floorbeams and to eliminate the possibility of the development of future cracking. The initial prototype, which was introduced on the west side of the northbound roadway at floorbeam FB77 was instrumented. Controlled load testing and monitoring of random traffic was conducted. However, the field measurements suggested that the initial retrofit geometry could be improved by making minor modifications to the prototype geometry. The modified retrofit was implemented at FB78 and additional measurements were made. This report summarizes the results of this work.

2.0 Instrumentation Plan and Data Acquisition

The instrumentation plan used for both the controlled truck testing and the uncontrolled monitoring is described in the following section. A detailed description of the location of the strain gages and the LVDT instrumented on the bridges could be found in Appendix A.

2.1 Strain Gages

Strain gages were installed at locations known to be subjected to higher stresses based on the FE analysis conducted by URS. In addition, gages were placed to establish the local response of the prototype retrofit and determine the effectiveness of the retrofit. Typical gage installation is shown in Figure 4.3.

Weldable and bondable uniaxial strain gages were used. The metal surfaces were ground and cleaned before installing the gages. After installation, gages were covered with multi-layer protective system and then sealed with silicon type agent.

The weldable gages were type LWK-06-W250B-350, with an active grid length of 0.25 inches. The “welds” are a point or spot resistance weld about the size of a pinprick. The probe is powered by a battery and only touches the foil that the strain gage

is mounted on by the manufacturer. This fuses a small pin size area to the steel surface. There are no arc strikes or heat-affected zones that are discernible produced by the spot welds. There is no preheat or any other preparation involved other than the preparation of the local metal surface by grinding and then cleaning before the gage is attached to the component with the welding unit. There has never been an instance of adverse behavior associated with the use of weldable strain gages including their installation on extremely brittle material such as A615 Gr75 steel reinforcing bars. The gages are a temperature-compensated uniaxial strain gage and perform very well when accurate strain measurements are required over long periods of time (months to years).

The bondable gages were type EA-06-125BZ-350 with an active grid length of 0.125 inches. They were installed on the metal surface at the desired location using a superglue type agent.

The gage resistance was 350Ω and an excitation voltage of 10 Volts was used. The gages were produced by Measurements Group Inc.

2.2 Displacement Sensors

A linear variable differential transformer (LVDT) was installed on the bridge to measure the relative displacement between the top flange of the floorbeam and the truss hanger. The measured displacement values were later correlated with the stresses measured by the strain gage data. The sensor is manufactured by Macro Sensors and has a displacement range of 1/4 inch with infinite resolution. The resolution of the measurement is limited by the data acquisition system. As configured during the testing and monitoring, the resolution of the LVDT was better than 0.1 mil. The LVDT installed at FB77 is shown in Figure 4.9.

2.3 Data Acquisition

A Campbell Scientific CR9000 Data Logger was used throughout the controlled load testing for the collection of the data. The logger is a high speed, multi-channel, 16-bit system configured with digital and analog filters to ensure a noise-free signal. By connecting a laptop computer to the logger, real-time data were viewed and permitted checkout of all sensors on site. Figure 2.1 shows the data acquisition system used including a differential LVDT power supply and uninterruptible power supply. The data logger, the differential LVDT power supply, and the uninterruptible power supply were enclosed in a weather-tight box for protection from harsh weather conditions. Power was provided by an existing 120 Volt source on the bridge.

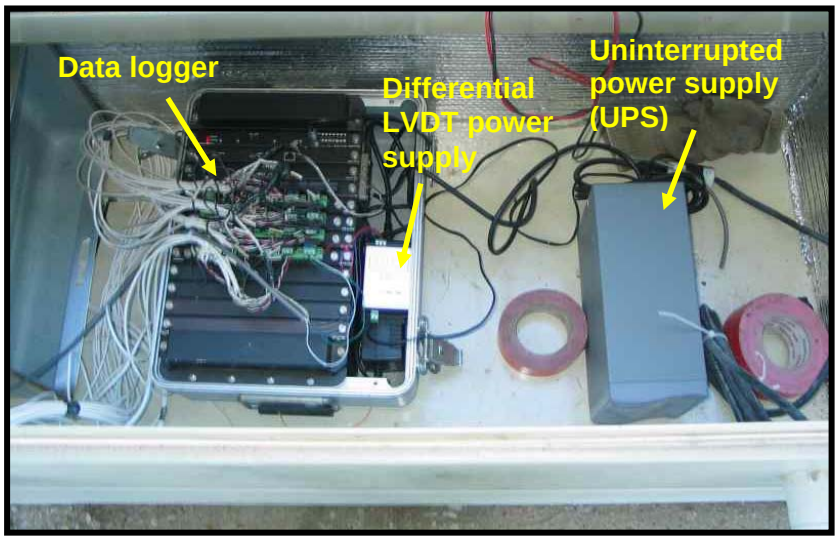

Figure 2.1 – Data acquisition system

2.4 Uncontrolled Monitoring

To minimize the volume of data collected, time history data were not collected continuously. Rather, the data acquisition system began recording when the stresses induced by live loads exceeded a predetermined stress threshold (i.e., a trigger) at a selected gage. The data acquisition system continuously monitored the strains in each gage and maintained a buffer of this data until the trigger event. Hence the entire event is recorded.

Stress-range histograms were also developed for all channels using the rainflow cycle-counting method. The histograms were generated continuously and did not operate on triggers, thus all cycles were counted. The histograms were updated every ten minutes. The stress-range bins were divided into 0.5 ksi intervals and cycles lass than 0.2 ksi were not counted.

3.0 Controlled Load Testing

A series of controlled load tests were conducted using the two test trucks shown in Figure 3.1. Both trucks had three main axles and one floating axle. Tests were conducted with both trucks having their floating axles in the "up" position. The trucks were loaded with gravel resulting in a gross vehicle weight (GVW) of 72,800 lb for the green truck (near truck in Figure 3.1) and GVW of 68,920 lb for the red truck (far truck in Figure 3.1). Figure 3.1 show both test trucks, while Figure 3.2 is a side view of the green test truck (the heavier truck). The geometry and the axle load data of red truck are listed in Table 3.1 and Table 3.2, respectively.

Figure 3.1 – Green and red test trucks used in the controlled load testing

Figure 3.2 – Side view of the test truck showing the floating axle in the up position

Test Description	Rear Axle Type	Front Axle Load (lb)	Rear axle group Load (lb)	GVW[1] (lb)	Date of Tests
Controlled Load Tests	Triaxle	15,000	57,800	72,800	October 7, 2004

Note:
1. GVW = Gross Vehicle Weight

Table 3.1 – Axle load data of the green test truck

Test Description	Rear Axle Type	Front Axle Load (lb)	Rear axle group Load (lb)	GVW[1] (lb)	Date of Tests
Controlled Load Tests	Triaxle	19,240	49,680	68,920	October 7, 2004

Note:
1. GVW = Gross Vehicle Weight

Table 3.2 – Axle load data for the red test truck

As previously mentioned, two retrofit prototypes were under investigation. The controlled load tests were conducted on the first retrofit prototype at FB77 on October 7, 2004 between 1 AM and 4:30 AM. Traffic on I-95 north was stopped by the Pennsylvania State Police approximately one mile south of the bridge. Stopping traffic was important to assure no disruption to the testing program by other vehicles crossing the bridge at the time of testing. After one test was completed, the test truck(s) were repositioned for the next test. During the time between tests, traffic was released.

Testing was not allowed on the west shoulder and portion of the west lane in the upper and lower decks as they were closed for maintenance. The remaining width of the bridge of both the upper and the lower decks, which included the east shoulder, the east lane, the middle lane and portion of the west lane was divided into three lanes (east lane, middle lane and west lane) to assure smooth traffic and to produce the same number of lanes as was the case before the required maintenance closure by the contractor.

It is important to note that the instrumented prototype details were located directly below the closed shoulder and portion of the west lane. Therefore, tests which were conducted over the west lane were not directly above the instrumented detail but as close to it as possible.

The tests consisted of a series of six dynamic tests and one crawl test. The dynamic tests were conducted on the upper and lower deck of the bridge using both test trucks separately. The traveling speed of the trucks varied between 40 to 55 miles per hour. Specifically, the first three dynamic tests were conducted with the 68,920 lb truck (lighter truck) traveling on the east lane of the upper deck at speed of 55 mph in the first test, on the center lane of the upper deck at speed of 43 mph in the second test, and on the west lane of the upper deck at speed of 55 mph in the third test. The fourth, fifth, and the sixth dynamic tests were conducted using the 72,800 lb test truck (heavier truck)

traveling over the lower deck in the east lane at speed of 40 mph, in the middle lane at speed of 42 mph and in the west lane at speed of 45 mph, respectively. The crawl test was conducted with both test trucks side-by-side traveling on the lower deck in the west and middle lane at a speed of 5 mph (the heavier truck was passing over the west lane and the lighter truck was passing over the middle lane). The speed, the direction, and the location of each truck for each test are listed in Table 3.3.

Test	Truck	Speed	Direction	Location	Notes
DYNTESTS.DAT	Lighter	Dynamic 55 mph	NB on SB lanes	East lane (upper deck)	NA
DYNTESTS.DAT	Lighter	Dynamic 43 mph	SB on SB lanes	Middle lane (upper deck)	NA
DYNTESTS.DAT	Lighter	Dynamic 55 Mph	NB on SB lanes	West lane (upper deck)	NA
DYNTESTS.DAT	Heavier	Dynamic 40 Mph	NB on NB lanes	East lane (lower deck)	NA
DYNTESTS.DAT	Heavier	Dynamic 42 Mph	NB on NB lanes	Middle lane (lower deck)	NA
DYNTESTS.DAT	Heavier	Dynamic 45 mph	NB on NB lanes	West lane (lower deck)	NA
CRL_TESTS.DAT	Both trucks	Crawl 5 mph	NB on NB lanes	side-by-side (West and middle lanes)	Heavier truck in west lane

Table 3.3 – Summary of controlled load tests

4.0 Summary of Instrumentation Layout

The following section summarizes the instrumentation plan for the bridge. Detailed instrumentation plan is provided in Appendix A.

4.1 Prototype retrofits

Two prototype retrofits schemes were proposed to engineers at PennDOT by the firm of URS. The retrofits were implemented at different floorbeams (FB77 and FB78). Instrumentation was installed at both floorbeams to investigate the performance of the retrofit. Figure 4.1 and 4.2 show both retrofits. Instrumentation of both retrofits will be discusses separately.

Figure 4.1 - Initial retrofit scheme at FB78 with the knee-brace removed and the cutout introduced in the web of FB78 (View looking south)

Figure 4.2 – Second retrofit scheme with knee-brace removed and the cutout introduced in the web of floorbeam FB78 as well as the back-to-back angle (View looking south)

4.2 Initial Retrofit - FB77

4.2.1 Strain Gages on the Web of the Floorbeam around the Cutout

Strain gages were installed on the web of the floorbeam around the cutout to monitor the stresses in the web. A total of 7 strain gages were installed on the web of floorbeam FB77 around the cut 1/4" away from the edge. Figure 4.3 shows the locations of CH_1, CH_3, CH_5, and CH_7. Channels CH_2, CH_4, and CH_6 were installed on the opposite face of the web directly behind the other channels (e.g., CH_2 is directly behind CH_1). A transverse stiffener attached to the other side of the web directly opposite to CH_7 did not allow for CH_8 to be installed back-to-back with CH_7.

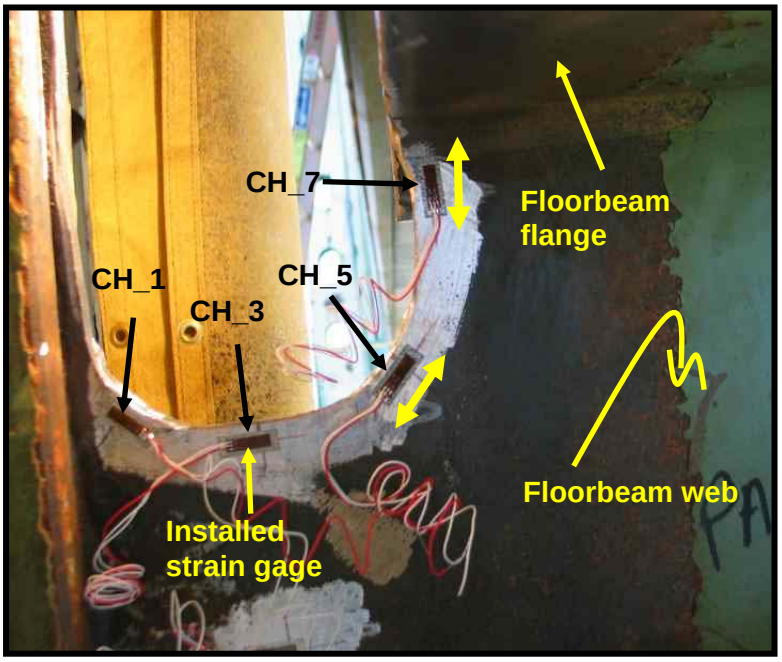

Figure 4.3 – Strain gages installed on the web around the cutout on the web of floorbeam FB77 (View looking north)

4.2.2 Strain Gages on Floorbeam Web below the Cutout at Longitudinal Stiffener Termination

Gages were also installed on the web of the floorbeam away from the cutout. The gages were installed to measure the stresses through a portion of the depth of the floorbeam below the cut. As shown in Figure 4.4, CH_13, CH_14, and CH_15 were installed on the web in-line with CH_3.

As part of the retrofit, the longitudinal stiffener welded to the web was cut back with a transitional radius to increase the fatigue resistance of the detail and to reduce the potential for future cracking. The stress range at the termination of the longitudinal stiffener after it has been cut was monitored using CH_11, which was installed on the web at the termination of the longitudinal stiffener. CH_12 was installed on the other side of the web directly opposite CH_11.

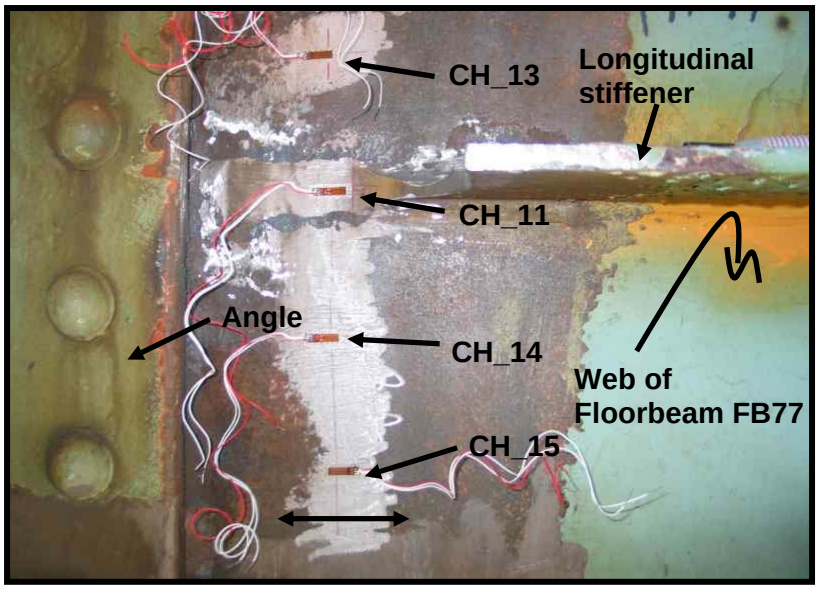

Figure 4.4 – CH_13, CH_14, and CH_15 installed on the web of floorbeam FB77 below the cutout in-line with CH_3 and CH_11 installed on the web at the termination of the longitudinal stiffener (View looking north)

4.2.3 Gage on the Web at Transverse Stiffener Detail

As shown in Figure 4.5, CH_8 was installed in the vertical direction on the web at the termination of the transverse stiffener to measure any out-of-plane bending of the web at floorbeam FB77 at this location. Since the stiffener is not rigidly attached to the top flange, the potential for cracking exists.

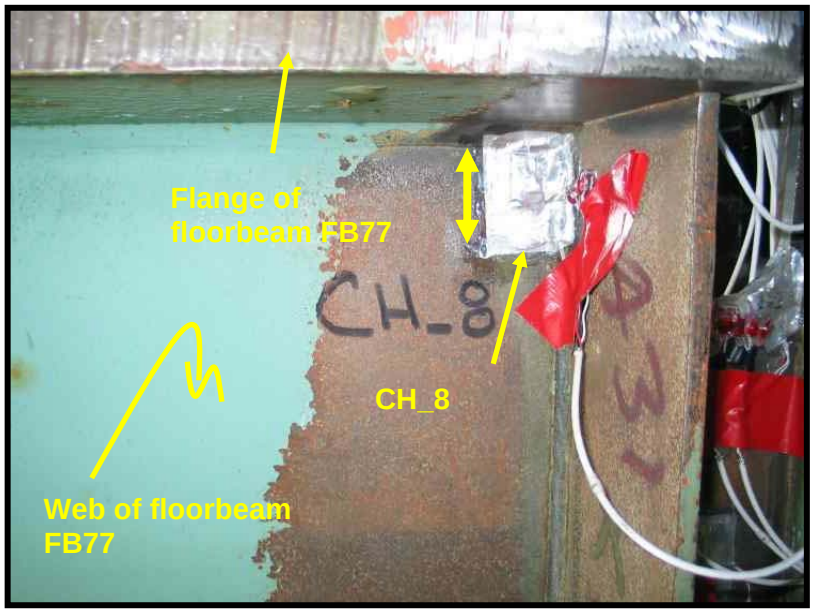

Figure 4.5 – CH_8 installed on the web of floorbeam FB77 at the web gap (View looking south)

4.2.4 Gage on the Web at Longitudinal Stiffener to Transverse Stiffener Detail

A strain gage was installed on the web of floorbeam FB77 to measure the stresses at the longitudinal stiffener to the transverse stiffener detail. Specifically, CH_10 was installed at the termination of the longitudinal stiffener next to the horizontal weld used for attaching the longitudinal stiffener and the vertical weld used for attaching the transverse stiffener. Figure 4.6 shows the location of the CH_10.

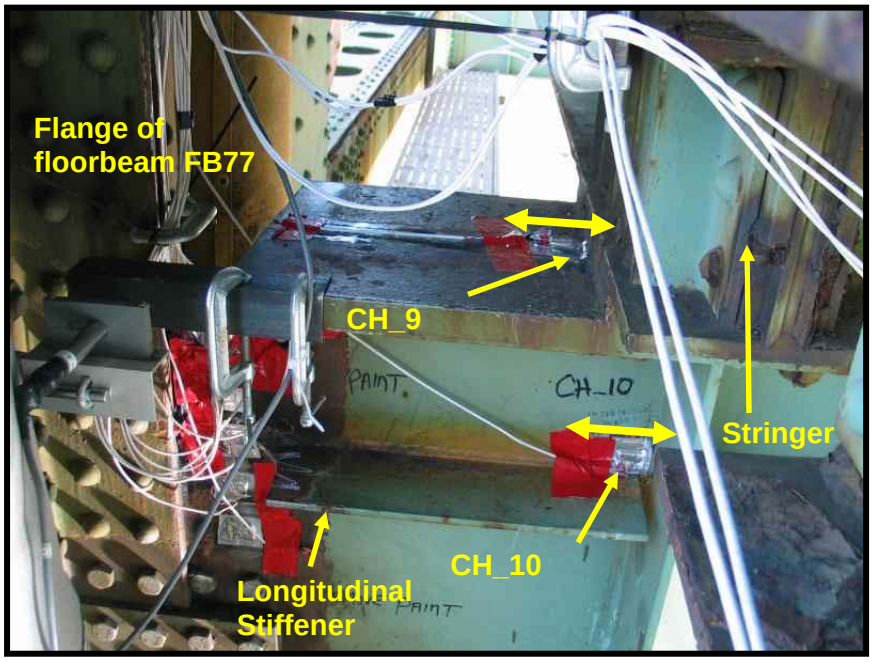

Figure 4.6 – CH_10 installed on the web of floorbeam FB77 at the longitudinal stiffener to transverse stiffener detail (view looking north)

4.2.5 Gages on Top and Bottom Flanges of the Floorbeam

Strain gages were installed on the top and bottom flanges of floorbeam FB77 to measure the primary or in-plane bending stresses. Specifically, CH_16 and CH_17 were installed at the centerline of the top and bottom flange respectively. The gages were placed 4'-8 ¾" away from the edge of the angle used for attaching the floorbeam to the truss hanger. Similarly, CH_18 and CH_19 were installed on the top and bottom flanges, respectively, at a distance 12'-5 ¼" away from the edge of the connection angle. Figure 4.7 shows CH_17, which was installed on the bottom flange of floorbeam FB77.

Another gage (CH_9) was also installed on the top flange of floorbeam FB77 at the floorbeam to the stringer intersection as shown in Figure 4.6. Note that the stringer is connected to the floorbeam by the means of bolts.

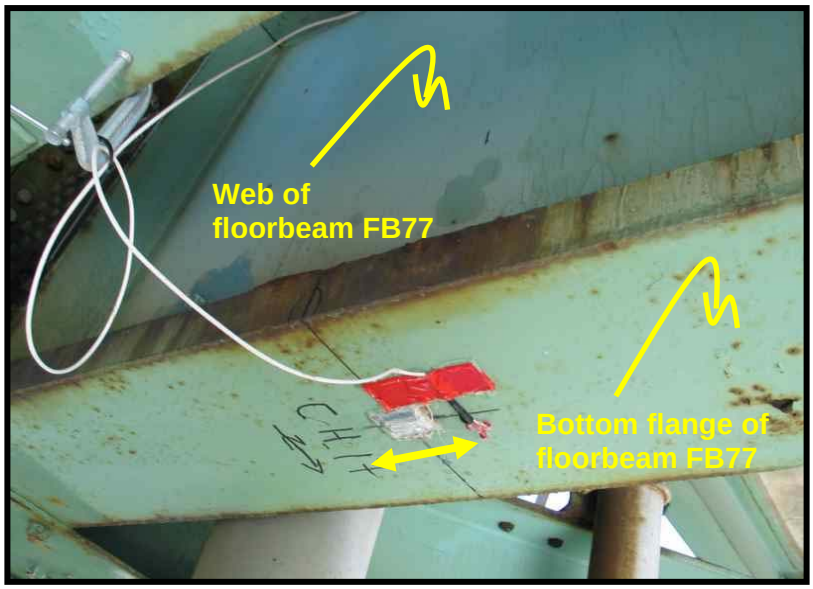

Figure 4.7 – CH_17 installed on the bottom flange of floorbeam FB77 at the longitudinal stiffener to transverse stiffener detail (view looking north)

4.2.6 Gages on Top and Bottom Flanges of the Stringer

Two gages were installed on the stringer located 25 feet east of the floorbeam to the truss hanger connection, 11 feet south of floorbeam FB77. The gages were installed to measure the magnitude of the stresses in the stringer flanges and to investigate the degree of composite action between the top flange of the stringer and the bridge deck. CH_21 was installed on the centerline of the bottom flange of the stringer, while CH_20 was installed on the bottom face of the top flange of the stringer. Channel CH_21 is shown in Figure 4.8

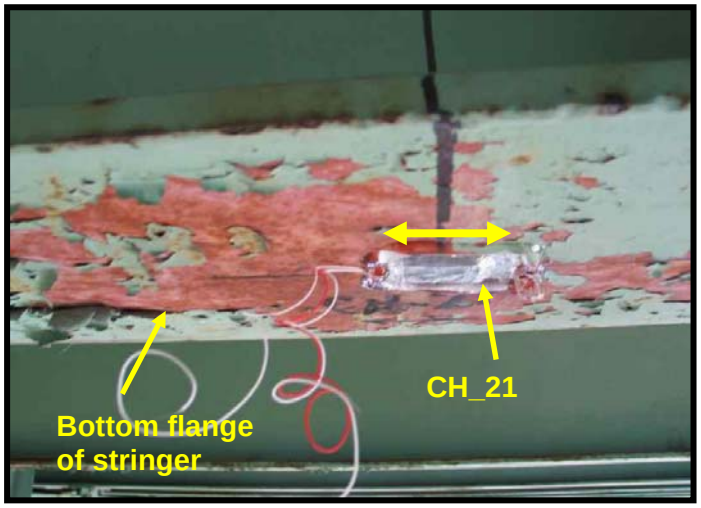

Figure 4.8 – CH_21 installed on the bottom flange of stringer the stringer located 25 feet east of the floorbeam to the truss hanger connection

4.2.7 Displacement Sensors

An LVDT was positioned to measure the relative horizontal displacement between the top flange of floorbeam FB77 and the vertical truss hanger. The sensor was mounted on the hanger as shown in Figure 4.9.

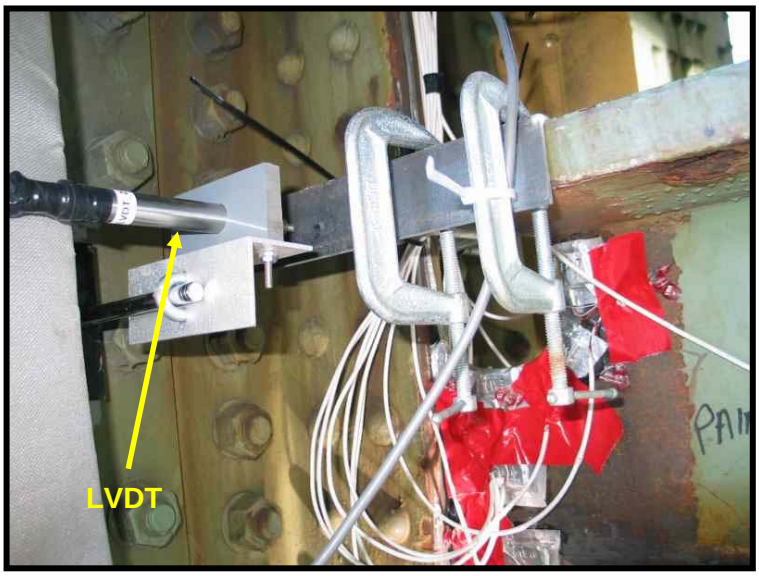

Figure 4.9 – Horizontal LVDT installed at floorbeam FB77

4.3 Initial Retrofit with Rivets Removed - FB77

Eighteen of the rivets used for connecting the angle to the floorbeam web and connection plate (previously in-place) were removed as shown in Figure 4.10. The rivets were removed to redirect the stress flow downward and away from the area of the web cut near the connection angles. The reduction in stress due to this modification was determined primarily by measurements made at CH_1 and CH_2 installed during the initial retrofit.

Figure 4.10 – Prototype retrofit at floorbeam FB77 with rivets removed

4.4 Modified Retrofit - FB78

Based on the measurements obtained from FB77 and previous experience with similar floorbeam cracking problems, it was concluded that making a relatively small modification to the geometry of the initial retrofit could potentially result in a significant decrease in the live load stress ranges at the details of concern. The second prototype retrofit strategy was incorporated at FB78. Additional instrumentation was added and measurements made.

4.4.1 Strain Gages on the Web of the Floorbeam around and below the Cutout

To assess the difference in the measured live load stresses between the initial retrofit at floorbeam FB77 and the modified retrofit at floorbeam FB78, channels CH_1 through CH_6 were installed on the web of floorbeam FB78 at similar locations where CH_1 through CH_6 were installed on floorbeam FB77. Channels CH_1 through CH_6 were installed on the web of floorbeam FB78, around the cut 1/4" away from the edge as shown in Figure 4.11. CH_2, CH_4, and CH_6 were installed on the opposite face of the web directly behind the previously installed channels (e.g., CH_2 is directly behind CH_1).

A strain gage (CH_7) was installed on the web of floorbeam FB78 approximately 3 ½" below CH_1. The channel was installed to measure the stress ranges in the lower portion of the web adjacent to the connection angles. At this location, net section stresses could be a concern if the magnitude of the stress range is too high. Although the largest stress ranges were expected at the edge of the cutout, higher stress ranges may exist below the cut due to restraint provided by the back-to-back connection angles. Hence, channel CH_7 was added to determine the stresses just below the cut.

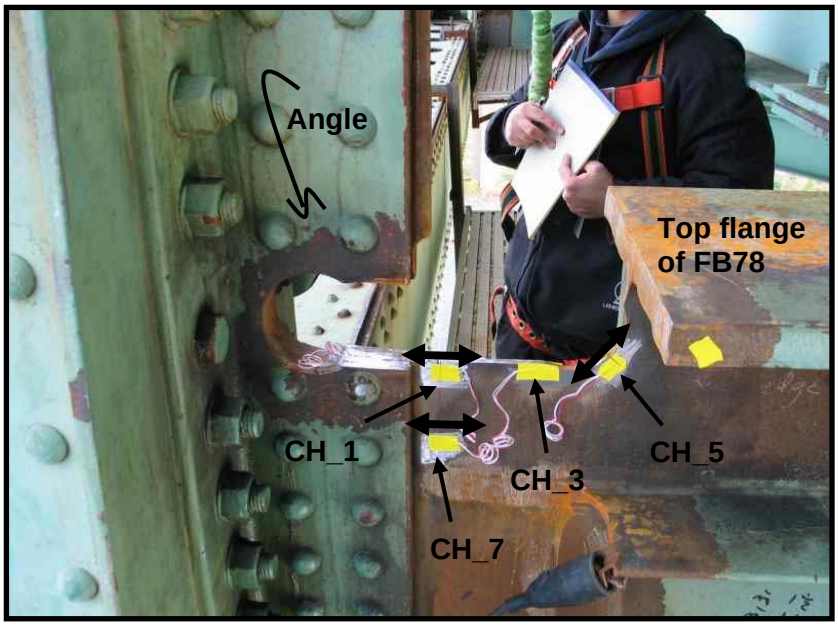

Figure 4.11 – Strain gages installed on the web around the cutout on the web of floorbeam FB78 (View looking north)

4.4.2 Strain Gages on the Web of the Floorbeam and the Angle Attaching the Floorbeam to the Truss Hanger

Two gages were installed on the web of the floorbeam and the angle attaching the floorbeam to the truss hanger. Specifically and as shown in Figure 4.12, CH_Web was installed on the web of the floorbeam (on the top face of the cut web) and CH_Angle was installed on the angle (on the top face of the cut angle). Both channels were installed to measure the stresses transferred from the web to the angles.

The geometry of the retrofit at FB78 allows a more uniform and smooth stress flow from the web into the connection angles. As the web passes between the angles, stress slowly leaves the web and is transferred into the angles. CH_Web was installed to verify that net section stresses were not unreasonably high and that stresses on the base metal of the web were also within reason. CH_Angle can be used to estimate the proportion of the stress in the web which has been "transferred" toe the angles and hence the effectiveness of the retrofit. In addition, the potential for net section cracking in the angles is identified.

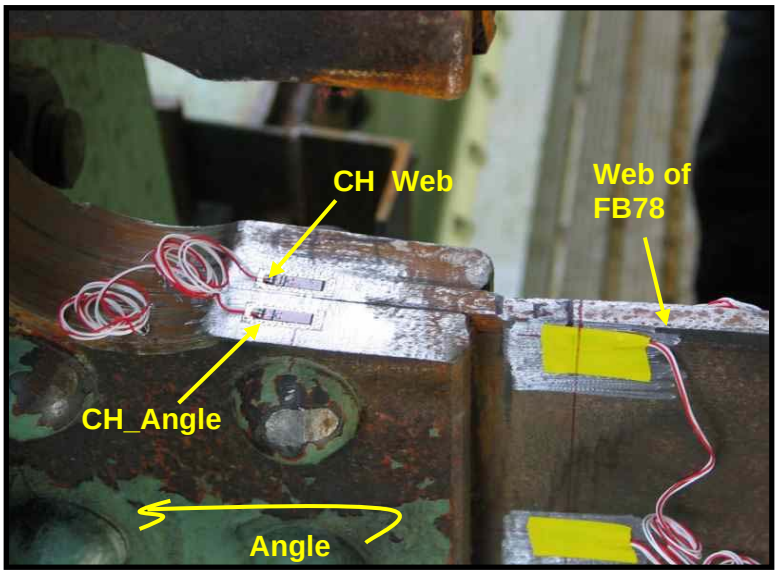

Figure 4.12 – Strain gages installed on the top face of the cut web and angle of Floorbeam FB78 (View looking north)

5.0 Results of Controlled Load Tests

Both crawl and dynamic tests were conducted on the first initial retrofit, which was implemented at floorbeam FB77. The results of the controlled crawl and dynamic load tests are discussed in this section.

5.1 Crawl Test

As previously mentioned, one crawl test (CRL_TEST) was conducted with both test trucks side-by-side traveling on the lower deck in the west and middle lane at a speed of 5 mph (the 72,800 lb truck was passing over the west lane and the 68,920 lb truck was passing over the middle lane). The discussion below pertains to the response of the instrumented details in the crawl test.

5.1.1 Stresses on the Floorbeam Web around the Cutout

CH_1 through CH_7 were installed on the web of floorbeam FB77, around the cutout. The gages were installed 1/4" away from the edge of the cut. Each pair of channels were installed back-to-back on the opposite face of the web (i.e. CH_2 is directly behind CH_1 and CH_4 is directly behind CH_3, etc.) A transverse stiffener on the opposite side of CH_7 did not allow for a gage to be installed directly opposite to CH_7. The channels were installed back-to-back to quantify the out-of-plane bending component that exists in the detail.

The detail where CH_1 through CH_6 were installed is classified as category A detail. The CAFL of the detail is 24 ksi. Channel CH_7 is however classified as category C detail. The CAFL of the detail is 10 ksi. The maximum response in all instrumented channels located around the cutout was measured in CH_2. Figure 5.1 shows the response of CH_1 and CH_2 (installed back-to-back) as both test trucks passed side-by-side in the west and middle lanes in the crawl test CRL_TEST. As can be seen in the figure a stress range cycle of approximately 27.5 ksi, which is higher than the CAFL of the detail was recorded by CH_2. Also as shown in the figure, both gages, CH_1 and CH_2 experienced an offset after the test truck passed over the detail (approximately 7.5 ksi for CH_2 and 4 ksi for CH_1). The offset is most likely attributed to a slip in the floorbeam to truss hanger connection. Such slip is not uncommon when a new or retrofit detail is heavily loaded for the first time and is referred to as “shakedown”. The test where two trucks passed side-by-side was easily the heaviest load the connection had been subjected to after the retrofit was completed. Hence, it is likely that some small “settling” of the connection took place.

A summary of the maximum, the minimum, and the stress range measured by the gages in the crawl test CRL_TEST is listed in Table 5.1. As listed in the table, high stress range values were recorded by some of the channels.

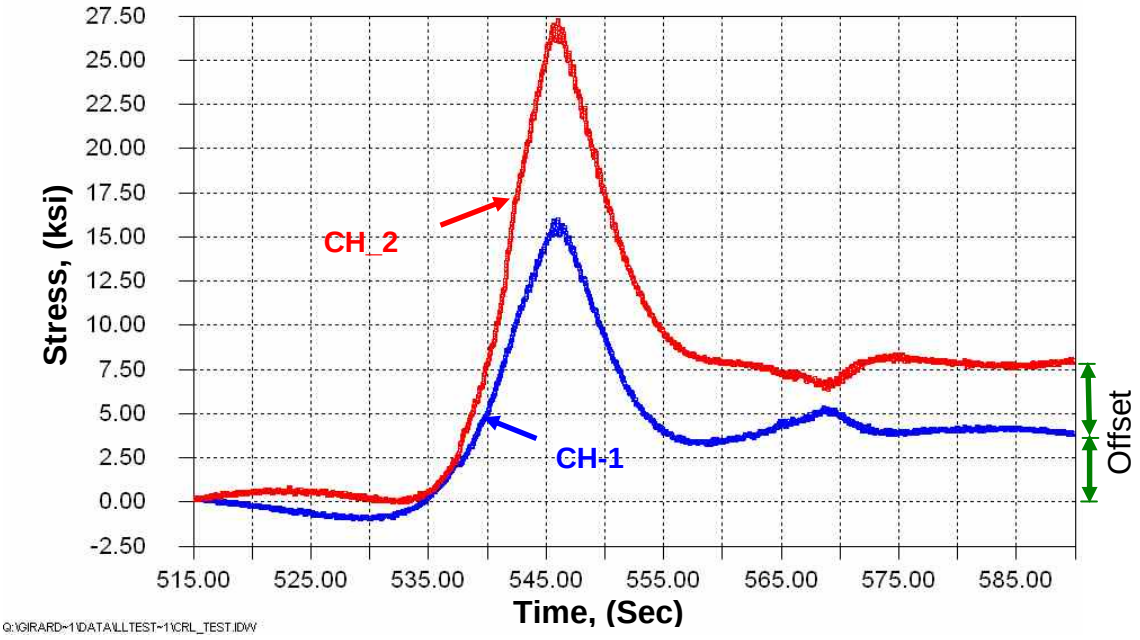

Figure 5.1 – Response of CH_1 and CH_2 installed 1/4 inch below the cutout of floorbeam FB77 as both test trucks drove side-by-side over the west and the middle lanes in the crawl test (CRL_TEST)

Channel	Trucks side-by-side		
	σ_{max}	σ_{min}	$\Delta\sigma$
CH_1	16.0	-1.1	17.1
CH_2	27.4	-0.1	27.5
CH_3	12.2	-0.4	12.6
CH_4	9.2	-0.3	9.5
CH_5	4.1	-1.9	6.0
CH_6	2.7	-1.5	4.2
CH_7	1.2	-0.6	1.8

Table 5.1 – Summary of peak measured stresses (ksi)
in the web of floorbeam FB77 around the cutout in the crawl test CRL_TEST

Out-of-plane bending stresses were calculated for CH_5 and CH_6 installed back-to-back on the below the cutout on the web of floorbeam FB77. The data used for generating the graphs where obtained from the dynamic test (DYN_TEST), since the crawl test results included an offset in the strain gages measurements after the test trucks passed over the details as described above. Figure 5.2 shows the in-plane and the out-of-plane components in the web below the cutout where CH_5 and CH_6 where installed.

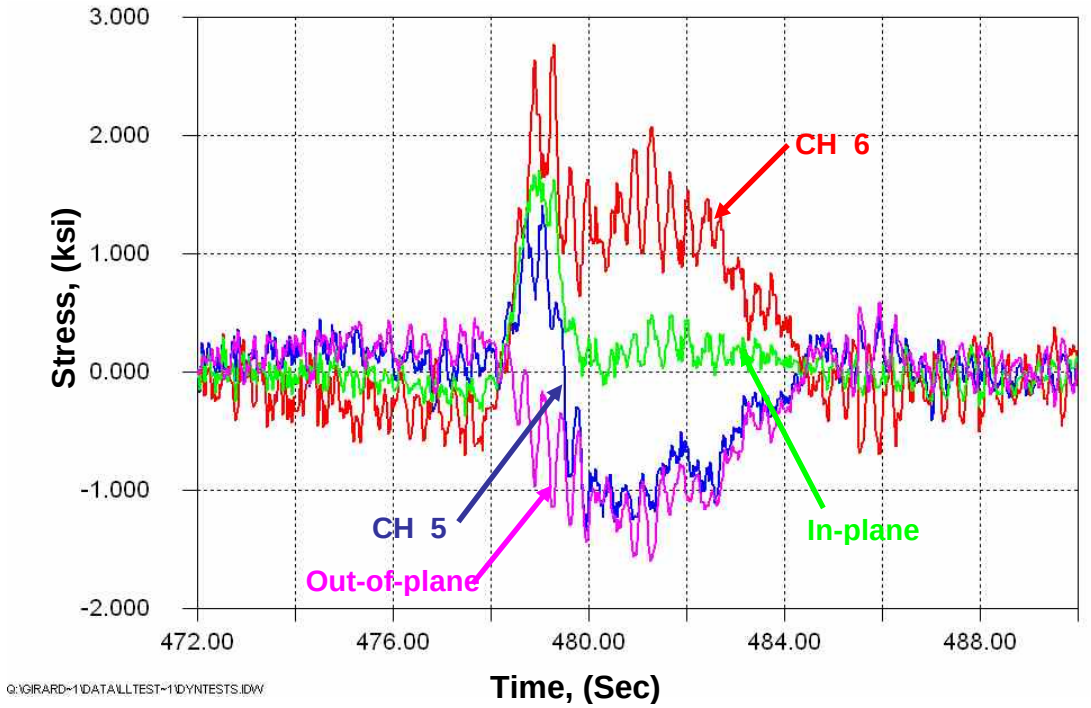

Figure 5.2 – Response of CH_5 and CH_6 installed back-to-back and the in-plane and the out-of-plane bending stress components 1/4 inch below the cutout of floorbeam FB77 as both test trucks drove side-by-side over the west and the middle lanes in the crawl test (CRL_TEST)

5.1.2 Stresses at Floorbeam Web below the Cutout at Longitudinal Stiffener Termination

As discussed before, CH_13, CH_14, and CH_15 were installed on the web of floorbeam FB77 away from the cutout and in-line with CH_3, to measure the stresses through a portion of the depth of the floorbeam below the cut. The detail where the channels were installed is classified as category A. The CAFL of category A is 24 ksi. Figure 5.3 shows the response of the three channels as both test trucks passed side-by-side in the crawl test CRL_TEST. The stress gradient, which exists through the instrumented portion of the web, is clearly shown in Figure 5.3 with the highest magnitude of stress recorded by CH_13 and the lowest by CH_15. A summary of the maximum, the minimum, and the stress range measured by the gages in the crawl test CRL_TEST is listed in Table 5.2. The listed values in the table indicate low magnitude of measured stress range. The highest magnitude of stress range measured was 5.2 ksi at CH_13, which is well below the CAFL of the detail.

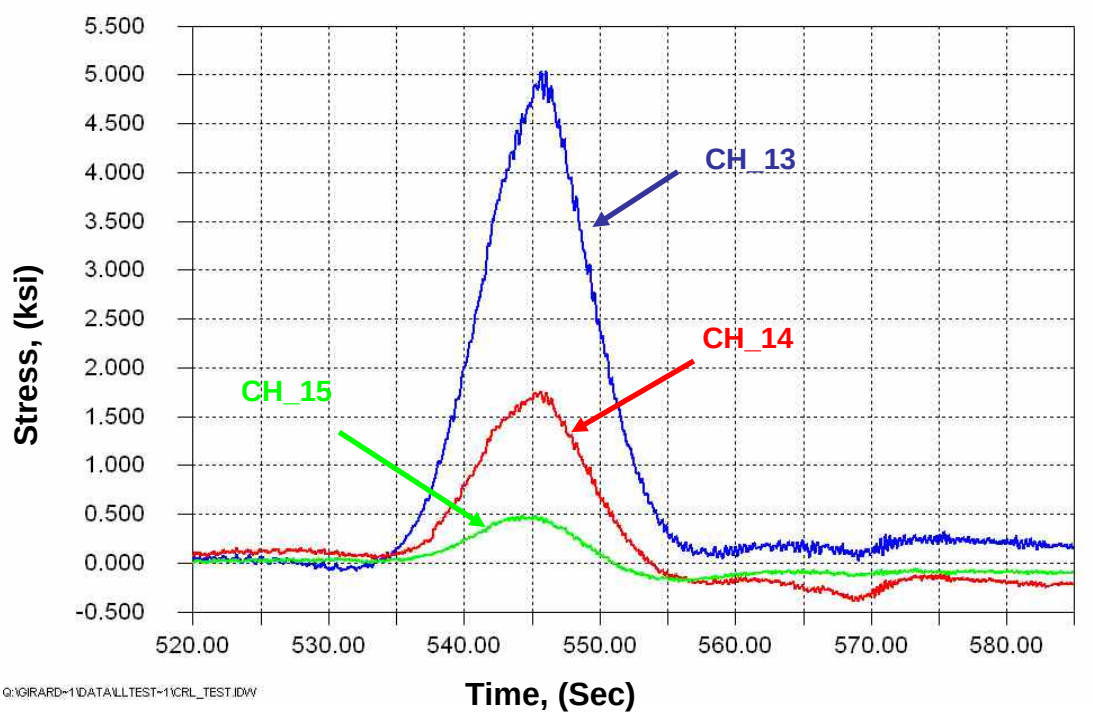

Figure 5.3 – Response of CH_13, CH_14, and CH_15 installed on the web of floorbeam FB77 away from the cutout and in-line with CH_3 as both test trucks drove side-by-side over the west and the middle lanes in the crawl test (CRL_TEST)

Channel	Trucks side-by-side		
	σ_{max}	σ_{min}	$\Delta\sigma$
CH_13	5.1	-0.1	5.2
CH_14	1.7	-0.2	1.9
CH_15	0.5	-0.2	0.7

Table 5.2 – Summary of peak measured stresses (ksi)
in the web of floorbeam FB77 below the cutout in the crawl test CRL_TEST

5.1.3 Stresses at the Web of the Floorbeam at Transverse Stiffener Detail

The response of the strain gage (CH_8) installed at the transverse stiffener detail is shown in Figure 5.4. The detail is classified as category detail C. The CAFL of the detail is 10 ksi. As shown in the figure, a low stress range value of 0.5 ksi was measured by the gage in the crawl test CRL_TEST. Table 5.3 lists the measured maximum, minimum, and the stress range recorded by the channel in the crawl test CRL_TEST.

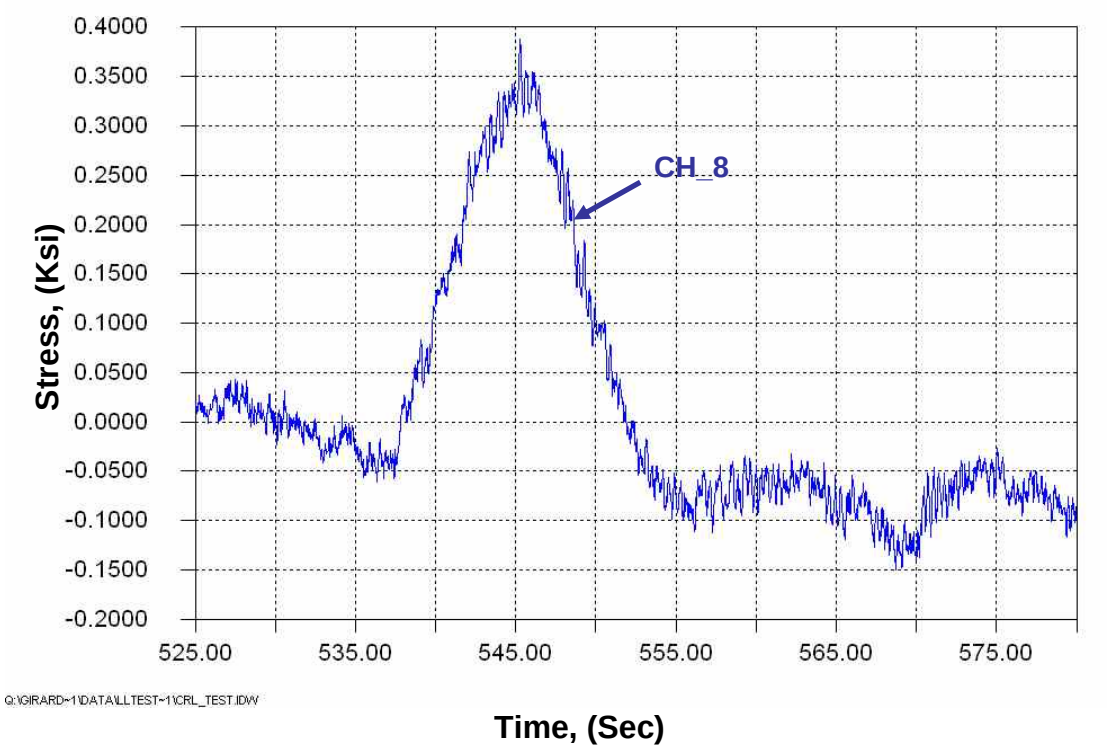

Figure 5.4 – Response of CH_8 installed on the web of floorbeam FB77 at a transverse stiffener detail as both test trucks drove side-by-side over the west and the middle lanes in the crawl test (CRL_TEST)

Channel	Trucks side-by-side		
	σ_{max}	σ_{min}	$\Delta\sigma$
CH_8	0.4	-0.1	0.5

Table 5.3 – Summary of peak measured stresses (ksi)
in the web of floorbeam FB77 at a transverse stiffener detail in the crawl test CRL_TEST

5.1.4 Stresses at Floorbeam Web below the Cutout at Longitudinal Stiffener Termination

The response of CH_11, which was installed to monitor the stress range at the termination of the longitudinal stiffener, is shown in Figure 5.5. Also shown in the figure is the response of CH_12, which was installed on the other side of the web, directly opposite of CH_11. The weld termination at channel CH_11 is classified as category detail E with a CAFL of 4.5 ksi. Channel CH_12 is classified as category A with a CAFL of 24 ksi. As indicated in the figure, the stress measured by CH_11 at the termination of the cutout was significantly higher than that recorded by CH_12, which was located on the other side of the web opposite of CH_11. Such difference in the magnitude of the measured stress was expected since some level of stress concentration exists at the termination of the longitudinal stiffener, where CH_11 was installed. The

difference of the magnitude of the measured stresses between CH_11 and CH_12 could also be attributed to an out-of-plane stress component, which when added to the in-plane component, causes the difference in the magnitude of the measured stress range between both faces of the web at the same cross section. The out-of-plane component is a result of a lateral shift in the vertical axis of bending in the web. Since the longitudinal stiffener is only on one side of the web, the vertical neutral axis is not located at the center of the web. Hence, out-of-plane bending is produced and will contribute to the difference in the observed response at CH_11 and CH_12. Similar to the discussion above, the offset in the strain gage measurements could be attributed to slipping in the floorbeam to truss hanger connection.

Summary of the measured maximum, minimum, and the stress range recorded by the channel in the crawl test CRL_TEST is listed in Table 5.4. The table shows in CH_11, stress range higher than the CAFL of the detail. No stress range measured at CH_11 was greater than the CAFL of the detail was however recorded where CH_12 was installed.

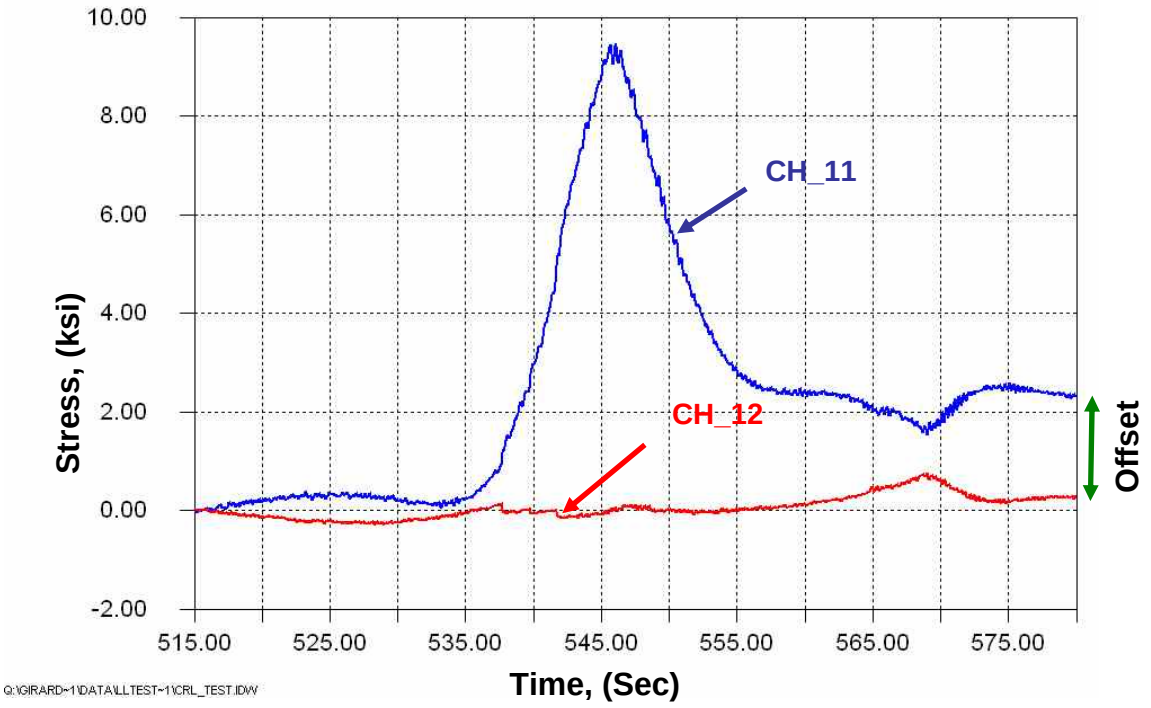

Figure 5.5 – Response of CH_11 installed on floorbeam web below the cutout at longitudinal stiffener termination as both test trucks drove side-by-side over the west and the middle lanes in the crawl test (CRL_TEST)

Channel	Trucks side-by-side		
	σ_{max}	σ_{min}	$\Delta\sigma$
CH_11	9.3	0.1	9.2
CH_12	0.7	-0.1	0.8

Table 5.4 – Summary of peak measured stresses (ksi)
in the web of floorbeam FB77 below the cutout at longitudinal stiffener termination in the crawl test CRL_TEST

5.1.5 Stresses at the Web at Longitudinal Stiffener to Transverse Stiffener Detail

The stress on the web at the longitudinal stiffener to transverse stiffener detail was recorded by CH_10. The detail is classified as category detail E with a CAFL of 4.5 ksi. As shown in Figure 5.6, the stress range measured at the detail in the crawl test (CRL_TEST) is approximately 3.2 ksi, which is below the CAFL of the detail. Table 5.5 lists the measured maximum, minimum, and stress range recorded by the channel in the crawl test CRL_TEST.

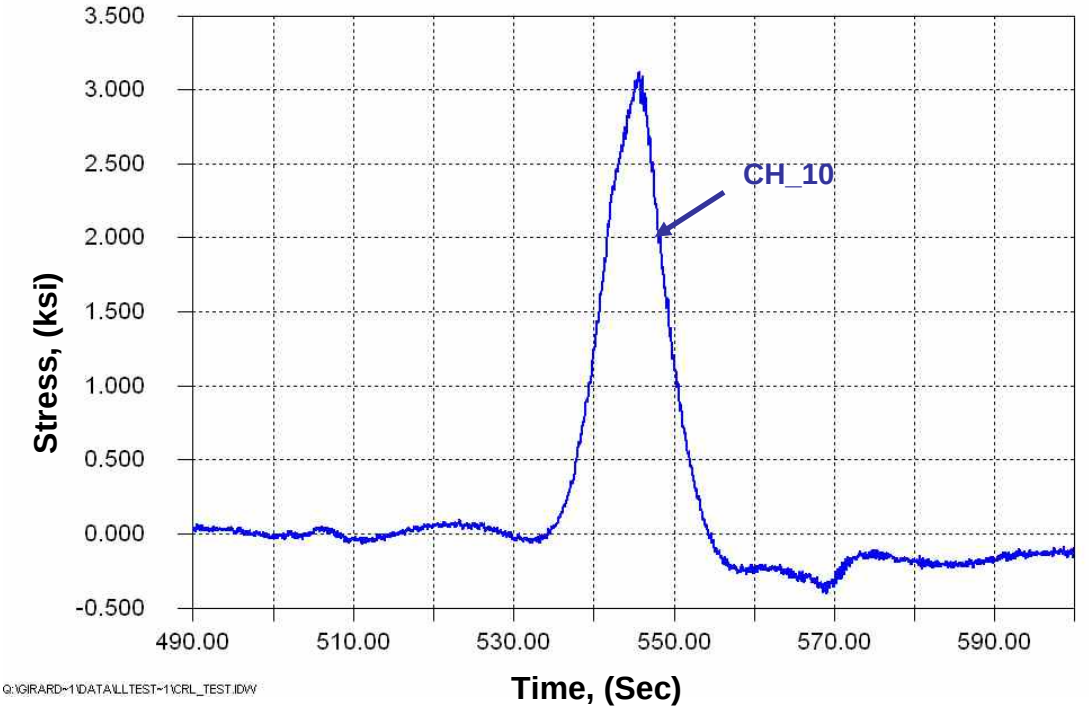

Figure 5.6 – Response of CH_10 installed on floorbeam web at longitudinal stiffener detail as both test trucks drove side-by-side over the west and the middle lanes in the crawl test (CRL_TEST)

Channel	Trucks side-by-side		
	σ_{max}	σ_{min}	$\Delta\sigma$
CH_10	3.1	-0.1	3.2

Table 5.5 – Summary of peak measured stresses (ksi)
in the web of floorbeam FB77 at longitudinal stiffener to transverse stiffener detail in the crawl test CRL_TEST

5.1.6 Stresses at Top and Bottom Flanges of the Floorbeam

Gages were installed on the top and bottom flange of floorbeam FB77 to measure the response of the floorbeam to a moving load with known weight and geometry. Specifically, CH_16 and CH_17 were installed on the top and bottom flange of the floorbeam, respectively at 4'-8 ¾" away from the edge of the angle used for connecting the floorbeam to the truss hanger. The other two gages (CH_18 and CH_19) were also installed on the top and bottom flange of the floorbeam, respectively at 12'-5 ¼" away from the edge of the angle used for connecting the floorbeam to the truss hanger.

The response of the four gages during the crawl test (CRL_TEST) is shown in Figure 5.7. As expected, CH_19 installed on the bottom flange measured tensile stresses, while CH_18 installed on the top flange measured compressive stresses. Simple beam theory suggests that both measured values however, should have been equal in magnitude and opposite in sign. It is however unclear as to why the measured stress in CH_19 was twice as much to what was measured in CH_18. The difference in the magnitude between measured stresses at both channels could be attributed to axial tension stresses introduced in the top flange of the floorbeam (along with the bending stresses). This was investigated using the limited data available. As shown in Figure 5.7, the axial stress component (i.e., the average of channels CH_18 and CH_19) was calculated. As can be seen, the magnitude of this component is small. Furthermore, since the axial force component would have to be essentially constant, the axial stresses at the gages near the connection (CH_16 and CH_17) where the flange is much thinner, would be much greater, which is not the case. Hence, it is not believed that there is a significant axial stress component in the floorbeam, which is consistent with other bridges instrumented. The effect is more likely due to some level of participation between the deck and the floorbeam. Hence, the deck, though connected with flexible stringers, is somewhat composite with the floorbeam. Similar behavior has been seen on other bridges.

Positive stresses were recorded by CH_16 installed on the top flange and CH_17 installed on the bottom flange in the same cross section. Intuitively it is expected that the stresses in CH_16 and CH_17 should be of equal magnitude and opposite signs. However, near a connection where only the web is attached, the stress flow does not necessarily follow can be easily predicted by beam theory. It is likely that some level of negative moment exists as evident by the tensile stresses exhibited by channels CH_1 and CH_2 as well as other channels on the web.

In short, the behavior near a connection is typically very complex and difficult to quantify with the limited instrumentation installed. Since the behavior of this portion of the floorbeam is not critical, it not be discussed further.

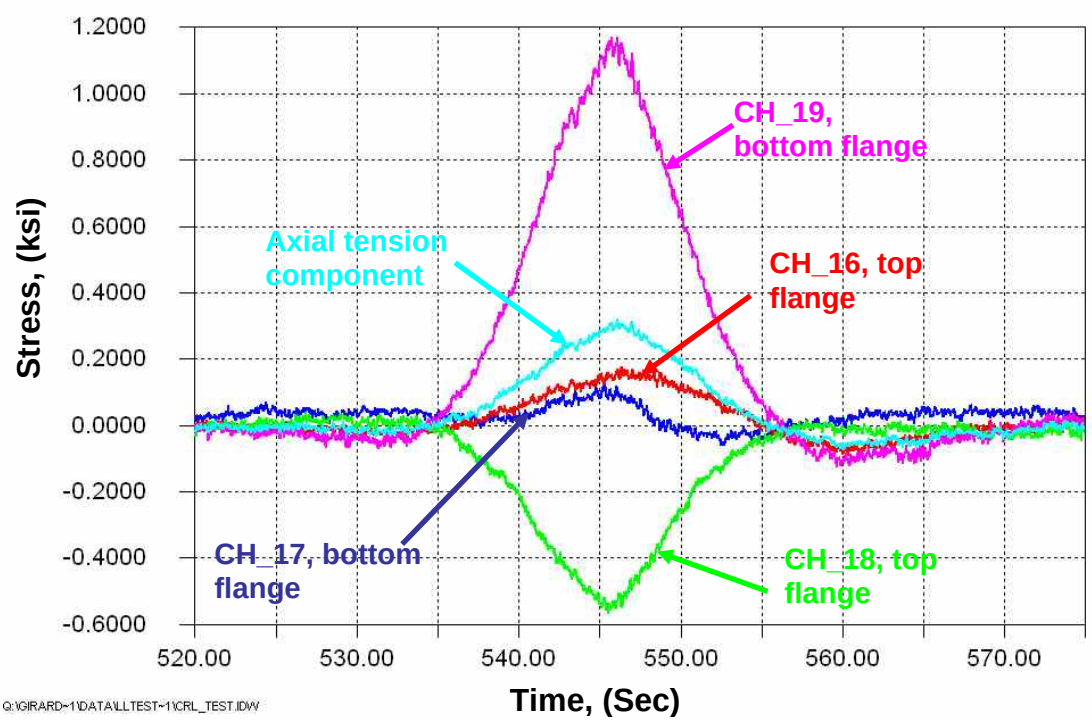

Figure 5.7 – Response of CH_16, CH_17, CH_18, and CH_19 installed on the top and bottom flange of floorbeam FB77 as both test trucks drove side-by-side over the west and the middle lanes in the crawl test (CRL_TEST)

Channel CH_9 was installed on the top flange of the floorbeam approximately 1'-2 11/16" away from the edge of the angle used for connecting the floorbeam to the truss hanger. The detail is conservatively classified as category detail E. The CAFL of the detail is 4.5 ksi. Figure 5.8 shows the response of CH_9 in the crawl test CRL_TEST. The magnitude of CH_9 appears to be slightly greater than expected, at least when compared to CH_16 and CH_17. The reason for this behavior is not known. A summary of the measured maximum, minimum, and the stress range recorded by CH_16, CH_17, CH_18, CH_19 and CH_9 in the crawl test CRL_TEST is listed in Table 5.6.

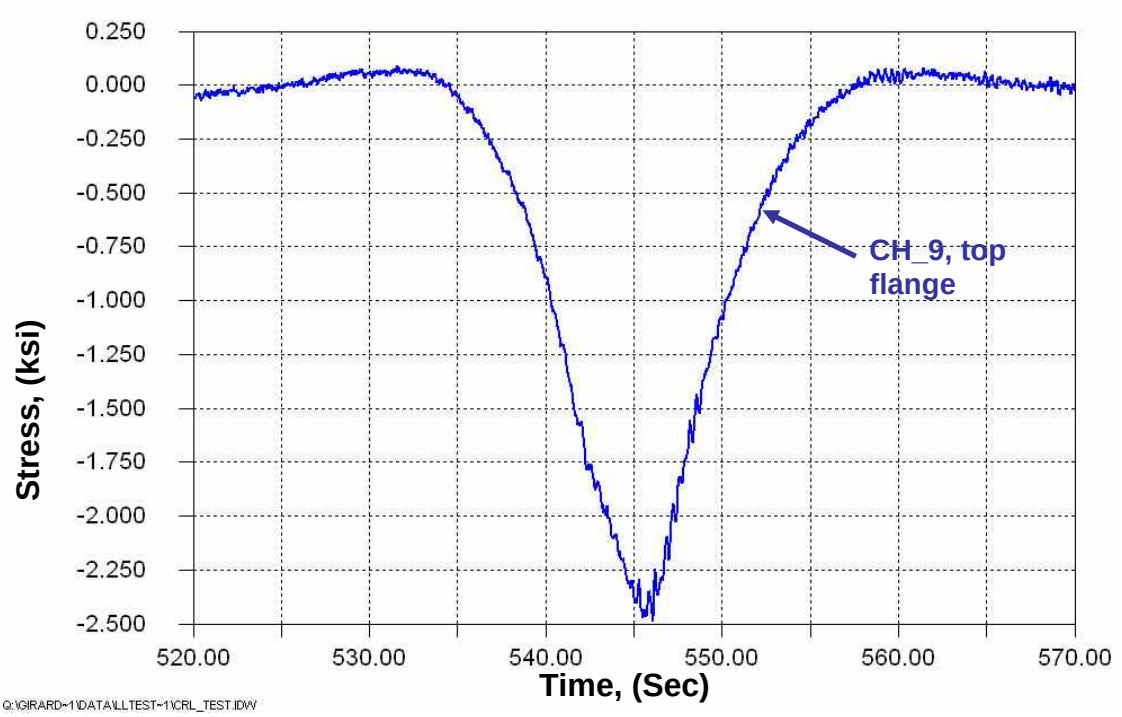

Figure 5.8 – Response of CH_9 installed on the top flange of floorbeam FB77 as both test trucks drove side-by-side over the west and the middle lanes in the crawl test (CRL_TEST)

Channel	Trucks side-by-side		
	σ_{max}	σ_{min}	$\Delta\sigma$
CH_16 (top flange)	0.1	-0.1	0.2
CH_17 (bottom flange)	0.2	-0.1	0.3
CH_18 (top flange)	0	-0.1	0.1
CH_19 (bottom flange)	1.1	-0.1	1.2
CH_9 (top flange)	0.1	-2.5	2.6

Table 5.6 – Summary of peak measured stresses (ksi) in the top and bottom flange of floorbeam FB77 at longitudinal stiffener to transverse stiffener detail in the crawl test CRL_TEST

5.1.7 Stresses at Top and Bottom Flanges of the Stringer

As previously discussed, strain gages (CH_20 and CH_21) were installed on the top and bottom flanges of the stringer located 25 feet east of the floorbeam (FB77) to the truss hanger connection to quantify the degree of composite action present between the stringers and the bridge deck and roughly estimate the transverse position of the trucks. Specifically, CH_20 was installed on the bottom face of the top flange of the stringer, while CH_21 was installed at the centerline of the bottom face of the bottom flange. The detail where the channels were installed is classified as category A (CAFL= 24 ksi).

Figure 5.9 shows the response of both channels to the moving load in the crawl test CRL_TEST. The figure shows a small magnitude of stress measured by CH_20 installed on the bottom face of the top flange of the stringer and higher magnitude of stress measured by CH_21 installed on the bottom flange of the stringer. The apparent difference in the magnitude in the stresses measured by both channels and the low magnitude of stress recorded by CH_20 suggests that high level of composite action is taken place between the stringer and the bridge deck. Note the local bending effects produced in the top flange as individual axles pass above the stringer.

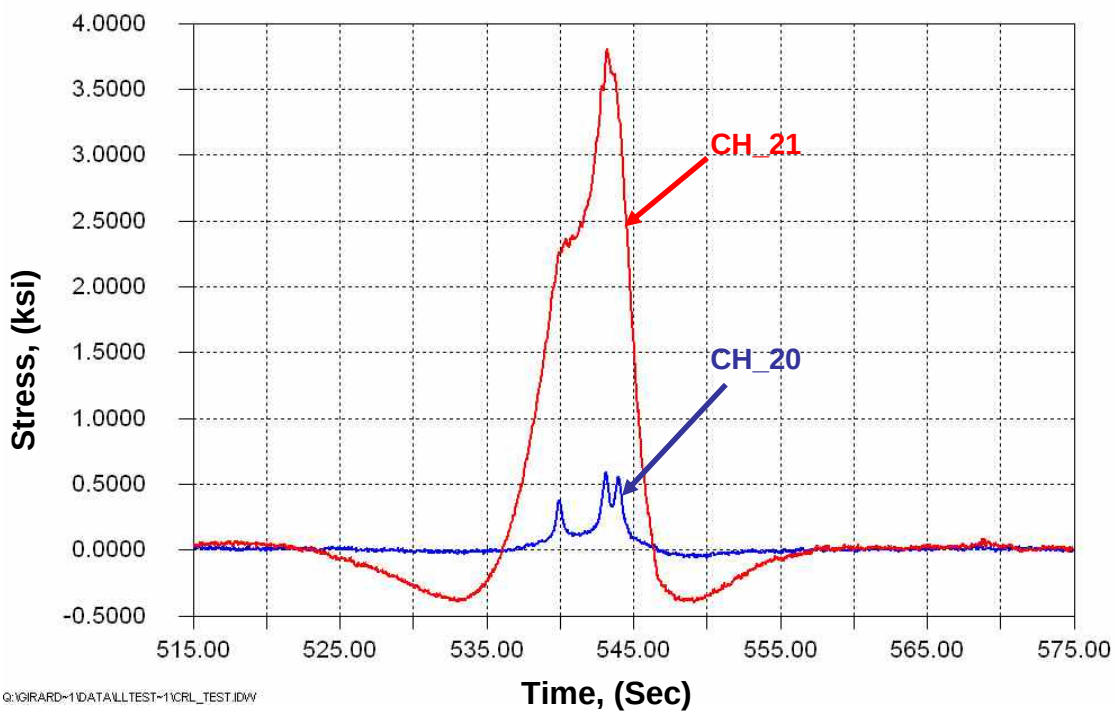

Figure 5.9 – Response of CH_20 and CH_21installed on the top and bottom flange of the stringer located 25 feet east of the floorbeam to the truss hanger connection as both test trucks drove side-by-side over the west and the middle lanes in the crawl test (CRL_TEST)

Channel	Trucks side-by-side		
	σ_{max}	σ_{min}	$\Delta\sigma$
CH_20	0.6	-0.1	0.7
CH_21	3.8	-0.4	4.2

Table 5.7 – Summary of peak measured stresses (ksi) in the top and bottom flange of the stringer located 25 feet east of the floorbeam to the truss hanger connection in the crawl test CRL_TEST

5.2 Dynamic Tests

As indicated before, six dynamic tests were conducted using each test truck separately in different lane positions for each test, where the heavier test truck was used for the dynamic testing on the lower deck and the lighter test truck was used for the dynamic testing on the upper deck. A description of the dynamic tests can be found in Chapter 3.

Dynamic vibration was observed at all instrumented channels. The intensity of the vibration was the highest as the lighter test truck passed over the upper deck and away from the detail (Figure 5.10) and was the lowest as the heavier test truck passed over the lower deck and directly over the detail (Figure 5.11). Below is a discussion on the response of the instrumented details to the moving load in each test.

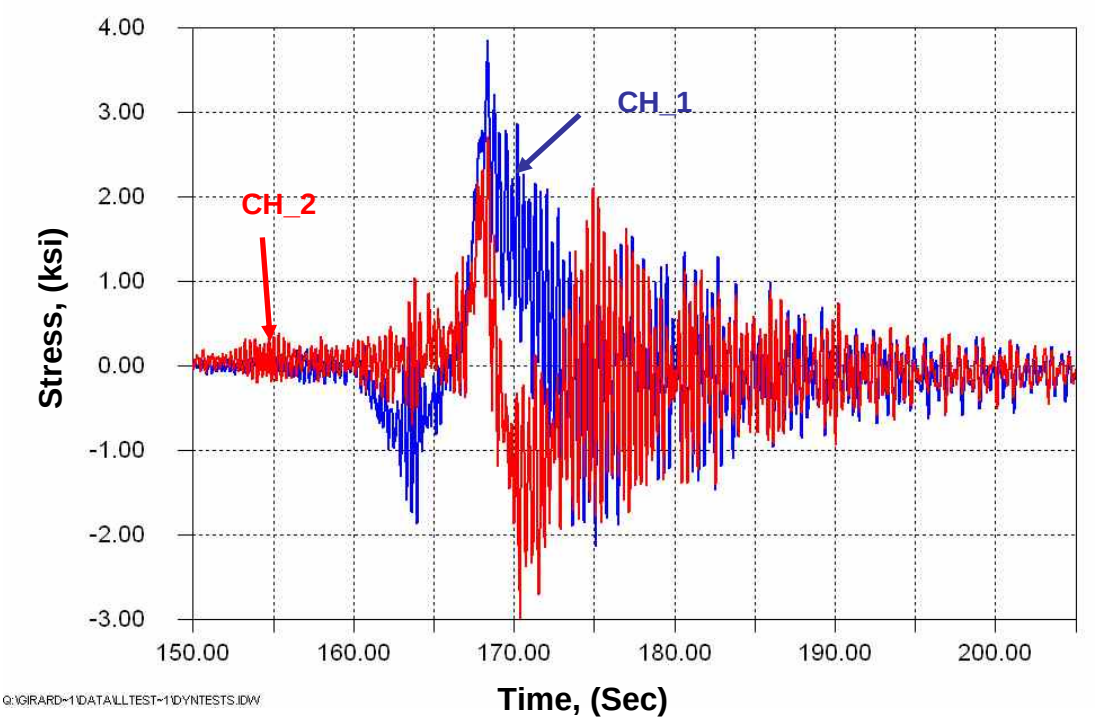

Figure 5.10 – Response of CH_1 and CH_2 installed 1/4 inch below the cutout of floorbeam FB77 as the lighter test truck passed over the upper deck in the east lane in the first dynamic test

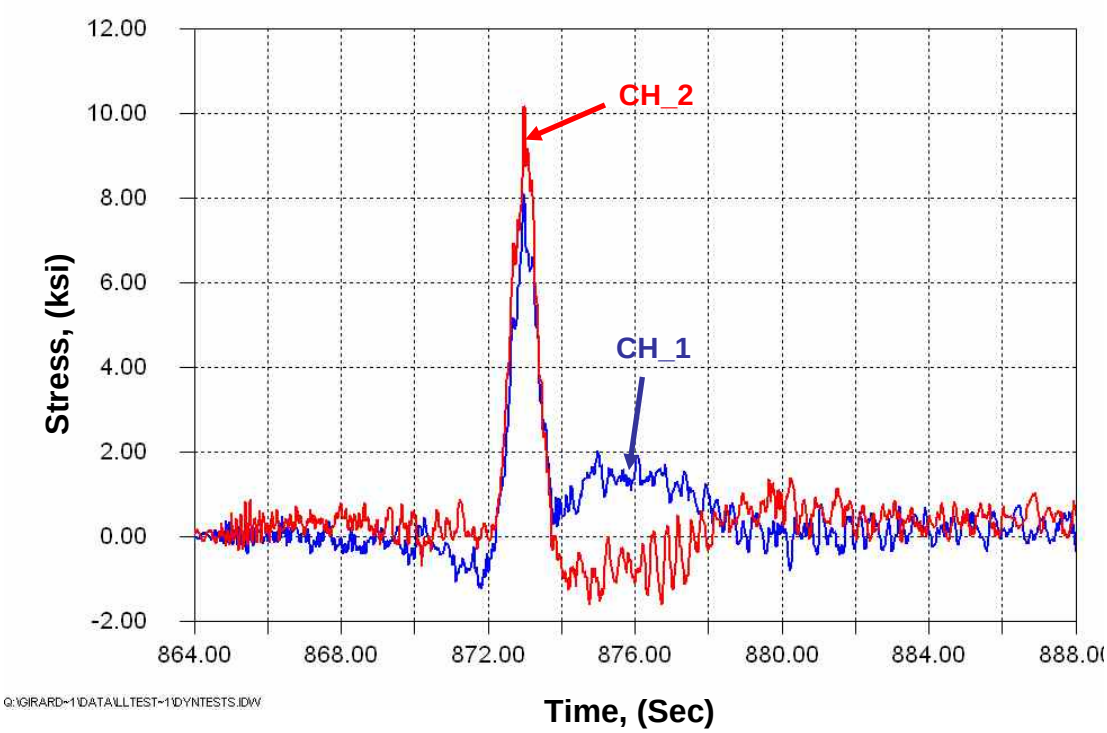

Figure 5.11 – Response of CH_1 and CH_2 installed 1/4 inch below the cutout of floorbeam FB77 as the heavier test truck passed over the lower deck in the west lane in the sixth dynamic test

5.2.1 Stresses on the Floorbeam Web around the Cutout

Table 5.8 summarizes the response of the channels installed on the web around the cutout in the dynamic tests. As indicated in the table, and for the most part, higher response was recorded when the heavier test truck was passing over the lower deck.

Truck in lane	(CH_1)			(CH_2)		
	σ_{max}	σ_{min}	$\Delta\sigma$	σ_{max}	σ_{min}	$\Delta\sigma$
NB on SB lanes, east lane (Lighter truck / upper deck)	3.3	-1.4	4.7	1.9	-1.8	3.7
SB on SB lanes, middle lane (Lighter truck / upper deck)	3.0	-0.6	3.6	1.6	-1.5	3.1
NB on SB lanes, west lane (Lighter truck / upper deck)	2.1	-0.5	2.6	1.2	-1.8	3.0
NB on NB lanes, east lane (Heavier truck / lower deck)	5.0	-0.9	5.9	5.5	-1.0	6.5
NB on NB lanes, middle lane (Heavier truck / lower deck)	7.5	-0.7	8.2	8.7	-2.0	10.7
NB on NB lanes, west lane (Heavier truck / lower deck)	8.1	-1.2	9.3	10.1	-1.2	11.3

Truck in lane	(CH_3)			(CH_4)		
	σ_{max}	σ_{min}	$\Delta\sigma$	σ_{max}	σ_{min}	$\Delta\sigma$
NB on SB lanes, east lane (Lighter truck / upper deck)	3.8	-0.7	4.5	4.1	-0.7	4.8
SB on SB lanes, middle lane (Lighter truck / upper deck)	2.9	0.0	2.9	2.7	0.0	2.7
NB on SB lanes, west lane (Lighter truck / upper deck)	2.1	-0.3	2.4	2.4	-0.3	2.7
NB on NB lanes, east lane (Heavier truck / lower deck)	4.9	-0.5	5.4	5.4	-0.5	5.9
NB on NB lanes, middle lane (Heavier truck / lower deck)	6.1	-0.5	6.6	6.7	-0.5	7.2
NB on NB lanes, west lane (Heavier truck / lower deck)	5.3	-0.5	5.8	6.1	-0.5	6.6

Truck in lane	(CH_5)			(CH_6)		
	σ_{max}	σ_{min}	$\Delta\sigma$	σ_{max}	σ_{min}	$\Delta\sigma$
NB on SB lanes, east lane (Lighter truck / upper deck)	1.8	-1.1	2.9	3.4	-1.1	4.5
SB on SB lanes, middle lane (Lighter truck / upper deck)	1.7	-1.2	2.9	3.0	-0.8	3.8
NB on SB lanes, west lane (Lighter truck / upper deck)	1.2	-1.2	2.4	2.5	-0.6	3.1
NB on NB lanes, east lane (Heavier truck / lower deck)	2.3	-0.7	3.0	3.4	-0.5	3.9
NB on NB lanes, middle lane (Heavier truck / lower deck)	2.6	-1.0	3.6	2.4	-0.9	3.3
NB on NB lanes, west lane (Heavier truck / lower deck)	1.6	-0.6	2.2	1.0	-0.9	2.0

Truck in lane	(CH_7)		
	σ_{max}	σ_{min}	$\Delta\sigma$
NB on SB lanes, east lane (Lighter truck / upper deck)	0.2	-0.6	0.8
SB on SB lanes, middle lane (Lighter truck / upper deck)	0.2	-0.4	0.6
NB on SB lanes, west lane (Lighter truck / upper deck)	0.1	-0.4	0.5
NB on NB lanes, east lane (Heavier truck / lower deck)	0.4	-0.5	0.9
NB on NB lanes, middle lane (Heavier truck / lower deck)	0.2	-0.5	0.7
NB on NB lanes, west lane (Heavier truck / lower deck)	0.7	-0.4	1.1

Table 5.8 – Summary of peak measured stresses (ksi)
in the web of floorbeam FB77 around the cutout in the dynamic tests DYNTESTS

5.2.2 Stresses at Floorbeam Web below the Cutout at Longitudinal Stiffener Termination

Stresses through a portion of the depth of the floorbeam below the cut were measured using CH_13, CH_14, and CH_15. Similar to the behavior observed during the crawl test, the highest magnitude of stress was recorded by CH_13 and the lowest by CH_15. Table 5.9 lists the summary of the maximum, the minimum, and the stress range recorded by the channels in the dynamic tests DYNTESTS.

Truck in lane	(CH_13)			(CH_14)		
	σ_{max}	σ_{min}	$\Delta\sigma$	σ_{max}	σ_{min}	$\Delta\sigma$
NB on SB lanes, east lane (Lighter truck / upper deck)	1.5	-0.5	2.0	0.4	-0.2	0.6
SB on SB lanes, middle lane (Lighter truck / upper deck)	1.1	-0.3	1.4	0.3	-0.3	0.6
NB on SB lanes, west lane (Lighter truck / upper deck)	0.9	-0.1	1.0	0.4	-0.3	0.7
NB on NB lanes, east lane (Heavier truck / lower deck)	2.0	-0.1	2.1	0.7	-0.3	1.0
NB on NB lanes, middle lane (Heavier truck / lower deck)	2.7	-0.2	2.9	1.0	-0.2	1.2
NB on NB lanes, west lane (Heavier truck / lower deck)	2.3	-0.3	2.6	0.7	-0.3	1.0

Truck in lane	(CH_15)		
	σ_{max}	σ_{min}	$\Delta\sigma$
NB on SB lanes, east lane (Lighter truck / upper deck)	0.3	0.0	0.3
SB on SB lanes, middle lane (Lighter truck / upper deck)	0.2	0.0	0.2
NB on SB lanes, west lane (Lighter truck / upper deck)	0.2	0.0	0.2
NB on NB lanes, east lane (Heavier truck / lower deck)	0.3	0.0	0.3
NB on NB lanes, middle lane (Heavier truck / lower deck)	0.3	0.0	0.3
NB on NB lanes, west lane (Heavier truck / lower deck)	0.1	-0.1	0.2

Table 5.9 – Summary of peak measured stresses (ksi)
in the web of floorbeam FB77 below the cutout in the dynamic test DYNTESTS

5.2.3 Stresses at the Web of the Floorbeam at Transverse Stiffener Detail

Low response was recorded in CH_ 8 during all dynamic tests as listed in Table 5.10.

Truck in lane	(CH_8)		
	σ_{max}	σ_{min}	$\Delta\sigma$
NB on SB lanes, east lane (Lighter truck / upper deck)	0.5	-0.1	0.6
SB on SB lanes, middle lane (Lighter truck / upper deck)	0.3	-0.1	0.4
NB on SB lanes, west lane (Lighter truck / upper deck)	0.2	-0.1	0.3
NB on NB lanes, east lane (Heavier truck / lower deck)	0.4	-0.1	0.5
NB on NB lanes, middle lane (Heavier truck / lower deck)	0.4	-0.1	0.5
NB on NB lanes, west lane (Heavier truck / lower deck)	0.0	-0.1	0.1

Table 5.10 – Summary of peak measured stresses (ksi)
in the web of floorbeam FB77 at a transverse stiffener detail in the dynamic test DYNTESTS

5.2.4 Stresses at Floorbeam Web below the Cutout at Longitudinal Stiffener Termination

As expected, the response of CH_11 was always higher than that of CH_12. However, the response of CH_11 was significantly higher than the response of CH_12 in the last two tests. This could be attributed to an increase in the local response (e.g., local our-of-plane web bending) of the detail as the test truck passes over the detail on the lower deck as previously discussed. The effect of the local response may diminish with the test truck passing away from the detail on the upper deck. Since the local effect is more driven by out-of-plane displacement produced by the eccentricity in the vertical neutral axis due to the one sided longitudinal stiffener, the effect would be less as the applied web stresses decrease. This can be idealized or thought of as similar to a P-Delta effect in which the local out-of-plane bending increases with increasing stress. The data are summarized in Table 5.11.

Truck in lane	(CH_11)			(CH_12)		
	σ_{max}	σ_{min}	$\Delta\sigma$	σ_{max}	σ_{min}	$\Delta\sigma$
NB on SB lanes, east lane (Lighter truck / upper deck)	1.1	-1.0	2.1	0.7	-0.3	1.0
SB on SB lanes, middle lane (Lighter truck / upper deck)	1.1	-1.0	2.1	0.6	-0.2	0.8
NB on SB lanes, west lane (Lighter truck / upper deck)	0.7	-0.9	1.6	0.6	-0.1	0.7
NB on NB lanes, east lane (Heavier truck / lower deck)	2.2	-0.6	2.8	0.8	-0.2	1.0
NB on NB lanes, middle lane (Heavier truck / lower deck)	3.6	-1.0	4.6	0.7	-0.2	0.9
NB on NB lanes, west lane (Heavier truck / lower deck)	3.1	-0.8	3.9	0.6	-0.2	0.8

Table 5.11 – Summary of peak measured stresses (ksi)
in the web of floorbeam FB77 below the cutout at longitudinal stiffener termination in the dynamic test DYNTESTS

5.2.5 Stresses at the Web at Longitudinal Stiffener to Transverse Stiffener Detail

The measured response of the detail was higher as the heavier test truck drove over the lower deck. The data are summarized in Table 5.12.

Truck in lane	(CH_10)		
	σ_{max}	σ_{min}	$\Delta\sigma$
NB on SB lanes, east lane (Lighter truck / upper deck)	0.6	-0.2	0.8
SB on SB lanes, middle lane (Lighter truck / upper deck)	0.4	-0.3	0.7
NB on SB lanes, west lane (Lighter truck / upper deck)	0.3	-0.2	0.5
NB on NB lanes, east lane (Heavier truck / lower deck)	1.1	-0.2	1.3
NB on NB lanes, middle lane (Heavier truck / lower deck)	1.6	-0.3	1.9
NB on NB lanes, west lane (Heavier truck / lower deck)	1.6	-0.2	1.8

Table 5.12 – Summary of peak measured stresses (ksi)
in the web of floorbeam FB77 at longitudinal stiffener to transverse stiffener detail in the dynamic test DYNTESTS

5.2.6 Stresses at Top and Bottom Flanges of the Floorbeam

Very low stresses were recorded in all five channels instrumented on the top and bottom flange of the floorbeam. As shown in Table 5.13, except for CH_9, all dynamic tests resulted in stress ranges well below 1 ksi.

Truck in lane	(CH_16)			(CH_17)		
	σ_{max}	σ_{min}	$\Delta\sigma$	σ_{max}	σ_{min}	$\Delta\sigma$
NB on SB lanes, east lane (Lighter truck / upper deck)	0.2	-0.1	0.3	0.0	-0.1	0.1
SB on SB lanes, middle lane (Lighter truck / upper deck)	0.2	0.0	0.2	0.0	-0.1	0.1
NB on SB lanes, west lane (Lighter truck / upper deck)	0.1	0.0	0.1	0.0	-0.1	0.1
NB on NB lanes, east lane (Heavier truck / lower deck)	0.2	0.0	0.2	0.0	-0.1	0.1
NB on NB lanes, middle lane (Heavier truck / lower deck)	0.2	0.0	0.2	0.0	0.0	0.0
NB on NB lanes, west lane (Heavier truck / lower deck)	0.0	-0.1	0.1	0.2	-0.1	0.3

Truck in lane	(CH_18)			(CH_19)		
	σ_{max}	σ_{min}	$\Delta\sigma$	σ_{max}	σ_{min}	$\Delta\sigma$
NB on SB lanes, east lane (Lighter truck / upper deck)	0.0	0.0	0.0	0.0	0.0	0.0
SB on SB lanes, middle lane (Lighter truck / upper deck)	0.0	0.0	0.0	0.0	0.0	0.0
NB on SB lanes, west lane (Lighter truck / upper deck)	0.0	0.0	0.0	0.0	0.0	0.0
NB on NB lanes, east lane (Heavier truck / lower deck)	0.0	0.0	0.0	0.0	0.0	0.0
NB on NB lanes, middle lane (Heavier truck / lower deck)	0.0	-0.1	0.1	0.4	0.0	0.4
NB on NB lanes, west lane (Heavier truck / lower deck)	0.0	-0.5	0.5	0.8	0.0	0.8

Truck in lane	(CH_9)		
	σ_{max}	σ_{min}	$\Delta\sigma$
NB on SB lanes, east lane (Lighter truck / upper deck)	0.2	0.0	0.2
SB on SB lanes, middle lane (Lighter truck / upper deck)	0.2	0.0	0.2
NB on SB lanes, west lane (Lighter truck / upper deck)	0.2	0.0	0.2
NB on NB lanes, east lane (Heavier truck / lower deck)	0.1	-0.3	0.4
NB on NB lanes, middle lane (Heavier truck / lower deck)	0.1	-1.0	1.1
NB on NB lanes, west lane (Heavier truck / lower deck)	0.1	-1.6	1.7

Table 5.13 – Summary of peak measured stresses (ksi)
in the top and bottom flange of floorbeam FB77 at longitudinal stiffener to transverse stiffener detail in the dynamic test DYNTESTS

5.2.7 Stresses at Top and Bottom Flanges of the Stringer

Although the bridge was designed as non-composite, the low magnitude of stresses measured by CH_20 installed on the bottom face of the top flange, clearly indicate a high degree of composite action between the stringer top flange and the concrete deck. Furthermore, the both CH_20 and CH_21 experienced no stresses as the lighter test truck passed over the upper deck, indicating that the stringer have very minimal response to moving loads on the upper deck as expected. The data are summarized in Table 5.14.

Truck in lane	(CH_20)			(CH_21)		
	σ_{max}	σ_{min}	$\Delta\sigma$	σ_{max}	σ_{min}	$\Delta\sigma$
NB on SB lanes, east lane (Lighter truck / upper deck)	0.0	0.0	0.0	0.0	0.0	0.0
SB on SB lanes, middle lane (Lighter truck / upper deck)	0.0	0.0	0.0	0.0	0.0	0.0
NB on SB lanes, west lane (Lighter truck / upper deck)	0.0	0.0	0.0	0.0	0.0	0.0
NB on NB lanes, east lane (Heavier truck / lower deck)	0.0	0.0	0.0	0.2	-0.1	0.3
NB on NB lanes, middle lane (Heavier truck / lower deck)	0.0	0.0	0.0	0.9	-0.2	1.1
NB on NB lanes, west lane (Heavier truck / lower deck)	0.4	0.0	0.4	2.9	-0.3	3.2

Table 5.14 – Summary of peak measured stresses (ksi)
in the top and bottom flange of the stringer located 25 feet east of the floorbeam to the truss hanger connection in the dynamic test DYNTESTS

6.0 Long-Term Monitoring

Ten strain gages of the twenty one installed on the bridge were chosen for long-term monitoring. As discussed before, two prototype retrofits schemes were proposed to engineers at PennDOT by the firm of URS. The first retrofit was implemented at floorbeam FB77, while the second at floorbeam FB78. The long-term monitoring of the first retrofit was conducted from October 8, 2004 until October 19, 2004 for a total of approximately 11 days. Some of the rivets used for the angle connection between the floorbeam web and the vertical truss hanger were removed as shown in Figure 4.10. Upon the removal of the rivets, monitoring of the retrofitted floorbeam FB77 continued from October 25, 2004 until November 1, 2004 for a total of approximately 7 days.

High stresses were recorded by the channels installed on the web of floorbeam FB77 next to the cutout. The measured stresses, although below the CAFL of the detail, were higher than anticipated and hence, of concern. As a consequence, a second prototype retrofit was proposed and implemented at floorbeam FB78. The prototype retrofit was monitored from November 1, 2004 till November 3, 2004 for approximately a day and half. The reason for monitoring the retrofit for such short period of time was because of the significant reduction in the magnitude of measured stress ranges around the cutout in the second prototype retrofit compared to the first prototype retrofit. It was clear very quickly that the modified retrofit at FB78 was a substantial improvement.

6.1 Results of Long-Term Monitoring

An estimate of the magnitude of stresses caused by the normal daily traffic could be established by reviewing the data collected during the monitoring period. Stresses of higher magnitude than produced by the test truck (s) were observed. Such an observation is not uncommon and is typically the result of multiple vehicles crossing the bridge.

6.1.1 Stresses in the Web of Floorbeam FB77 around the Cutout – Initial Retrofit

As previously mentioned, seven gages (CH_1 through CH_7) were installed on the web of floorbeam FB77 around the cutout. The web plate where the channels were installed could be classified as a category A per AASHTO specifications. No stress-range cycles higher than the CAFL of the detail were measured by any of the channels during the monitoring period. However, as mentioned before, the stresses were higher than desired and were a cause of a concern. Figure 6.1 shows the stress-range histogram for CH_1 and CH_2 installed on the web of the cutout of floorbeam FB77 (first retrofit). The general shape of the histogram for Channels CH_1 and CH_2 can be considered typical for other gages, although the magnitude of the counts in each bin is different.

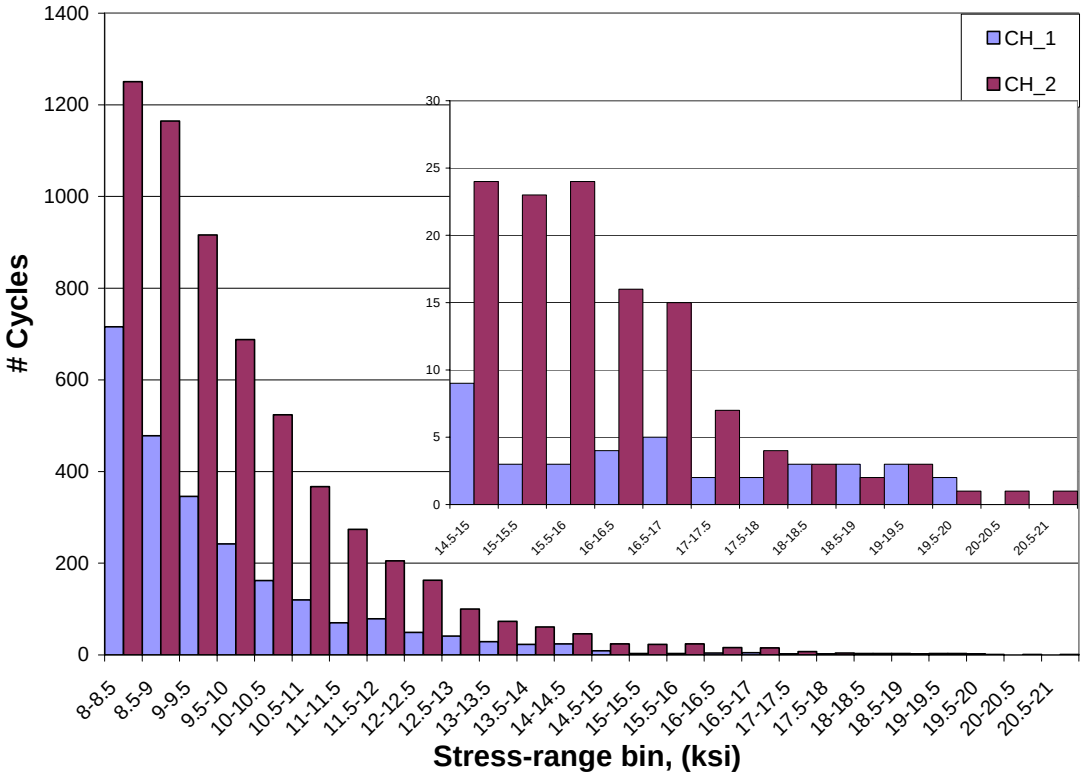

Figure 6.1 – Stress-range histogram for channels CH_1 and CH_2

As indicated in the figure, CH_2 experienced a higher count in each bin than CH_1 for a given stress range. The inset in the figure is a magnification of the last portion of the figure. Stress-range cycles as high as 19.75 ksi and 20.75 ksi were measured by CH_1 and CH_2, respectively. A lower-bound stress range truncation level of 8 ksi was selected for producing the histogram. Typically for fatigue evaluation, the truncation level is 1/4 to 1/3 times the CAFL of the detail.

A summary of the magnitude of the maximum stress range, effective stress range, number of cycles measured per day, and the estimated remaining fatigue life for the details is presented in Table 6.1. As can be seen in the table, the fatigue life calculations indicate an infinite life for all four instrumented locations along the cut. The only detail where finite life was not achieved was at the termination of the longitudinal stiffener. However, as discussed in Section 6.1.3, the second retrofit strategy reduced stresses at this location to levels where infinite life is expected. Where a fatigue life of "Over 100" years is listed, the calculated life was greater than 100 years. The actual calculated life is usually substantial greater, sometimes several thousand years.

Channel	Fatigue Life Calculation Summary - Initial Retrofit FB77							
	S_{rmax} (ksi)	Cycles > CAFL		S_{reff} (ksi)	Cycles / Day	Remaining Life (Years)	Category	Location
		#	%					
CH_1	19.75	0	0.00	9.9	215	Infinite	A	Around the cutout
CH_2	20.75	0	0.00	10.1	530	Infinite	A	Around the cutout
CH_3	13.75	0	0.00	9.4	131	Infinite	A	Around the cutout
CH_4	13.25	0	0.00	9.3	85	Infinite	A	Around the cutout
CH_5	11.75	0	0.00	8.9	7	Infinite	A	Around the cutout
CH_6	19.25	0	0.00	12.2	43	Infinite	A	Around the cutout
CH_7	8.25	0	0.00	5.4	27	Infinite	C	Around the cutout
CH_9	3.75	0	0.00	2.1	141	Infinite	E	Top flange of floorbeam FB77
CH_10	5.75	2	0.04	1.9	498	Over 100	E	Long. stiffener to tans. stiffener detail
CH_11	11.75	2199	3.27	2.7	6,002	25.5	E	Long. stiffener termination

Notes:
1. Details with S_{rmax} less than the stress truncation level used for the fatigue calculations are assigned 0 cycles/day and subsequently an infinite fatigue life.
2. Remaining life assumes time equal to zero starts in 2004 where original base material was removed during retrofit since previous fatigue damaged areas have been removed.

Table 6.1 – Summary of fatigue life calculations of the initial retrofit at floorbeam FB77 with rivets removed. CH_1 through CH_7 were installed on the web of floorbeam FB77 around the cutout, and CH_10 was installed at the longitudinal stiffener to transverse stiffener detail, and CH_11 was installed at the termination of the longitudinal stiffener

6.1.2 Stresses in the Web of Floorbeam FB77 around the Cutout – Initial Retrofit with Rivets Removed

Eighteen of the rivets used in the angle connection between the web of floorbeam FB77 and the truss hanger were removed to redirect the stress flow from the floorbeam to the connection angles and reduce the magnitude of the stress measured by CH_1 and CH_2 in the initial retrofit.

As shown in Table 6.2, the removal of the rivets resulted in a predicted fatigue life is infinite at all channels except for CH_10 and CH_11. Furthermore, with the exception of CH_5 and CH_11, the maximum measured stress ranges were not significantly lower than what were measured in the initial retrofit with the rivets in place. In other words, the removal of the rivets had little impact on the predicted fatigue life and resulted in no significant reduction to the maximum measured stresses. However, the number of cycles per day was noticeable less after the rivets were removed which suggests that the removal was effective in "shifting" the histogram somewhat. Nevertheless, the small beneficial effect resulting from the removal of the rivets prompted the proposal of an alternative retrofit scheme that could significantly reduce the maximum measured stresses around the web of the cutout.

It is also important to mention that if the initial retrofit was to be implemented, the existence of any nocks or gouges that were not ground smooth (by mistake) would likely have resulted in cracking due to the higher stress ranges. Although quality is critical in any retrofit strategy, the geometry proposed at FB78 will be less sensitive to any imperfections in the surface of the cut edge. It was therefore felt important to implement a second retrofit scheme (Floorbeam FB78) to try and significantly reduce the measured live load stresses on the web around the cutout.

Channel	Fatigue Life Calculation Summary - Initial Retrofit FB77, with Rivets Removed							
	S_{rmax} (ksi)	Cycles > CAFL		S_{reff} (ksi)	Cycles / Day	Remaining Life (Years)	Category	Location
		#	%					
CH_1	18.25	0	0.00	9.5	37	Infinite	A	Around the cutout
CH_2	15.25	0	0.00	9.4	97	Infinite	A	Around the cutout
CH_3	11.25	0	0.00	9.0	26	Infinite	A	Around the cutout
CH_4	11.75	0	0.00	9.0	10	Infinite	A	Around the cutout
CH_5	12.75	0	0.00	11.0	1	Infinite	A	Around the cutout
CH_6	13.75	0	0.00	13.0	9	Infinite	A	Around the cutout
CH_7	9.25	0	0.00	6.5	13	Infinite	C	Around the cutout
CH_10	6.75	4	0.20	1.9	360	Over 100	E	Long. stiffener to tans. stiffener detail
CH_11	11.75	997	2.80	2.9	5,246	23.6	E	Long. stiffener termination

Notes:
1. Details with S_{rmax} less than the stress truncation level used for the fatigue calculations are assigned 0 cycles/day and subsequently an infinite fatigue life.
2. Remaining life assumes time equal to zero starts in 2004 where original base material was removed during retrofit since previous fatigue damaged areas have been removed.

Table 6.2 – Summary of fatigue life calculations of the initial retrofit at floorbeam FB77 with rivets removed. CH_1 through CH_7 were installed on the web of floorbeam FB77 around the cutout, and CH_10 was installed at the longitudinal stiffener to transverse stiffener detail, and CH_11 was installed at the termination of the longitudinal stiffener

6.1.3 Stresses in the Web of Floorbeam FB78 around the Cutout – Second Retrofit

As indicated in Table 6.3, the maximum stress-range cycles measured by channels CH_1 through CH_5 installed around the cutout of floorbeam FB78 was significantly lower than what was measured by CH_1 through CH_5, installed at the same location on the web of floorbeam FB77 (Table 6.2).

In addition to the comparison made between Table 6.2 and Table 6.3, CH_1 and CH_2 installed on the web of floorbeam FB77 were monitored concurrently with the channels installed and monitored on floorbeam FB78. As shown in Table 6.3, the second retrofit was capable of reducing the maximum measured stresses in CH_1 and CH_2 by approximately 50%.

Channel	Fatigue Life Calculation Summary – Second Retrofit FB78							
	S_{rmax} (ksi)	Cycles > CAFL		S_{reff} (ksi)	Cycles / Day	Remaining Life (Years)	Category	Location
		#	%					
CH_1	8.75	0	0.00	8.75	1	Infinite	A	Around the cutout
CH_2	7.75	0	0.00	Note 1	0	Infinite	A	Around the cutout
CH_3	5.75	0	0.00	Note 1	0	Infinite	A	Around the cutout
CH_4	6.25	0	0.00	Note 1	0	Infinite	A	Around the cutout
CH_5	6.75	0	0.00	Note 1	0	Infinite	A	Around the cutout
CH_6	10.25	0	0.00	8.7	11	Infinite	A	Around the cutout
CH_7	11.25	0	0.00	9.7	4	Infinite	A	Around the cutout
Web	7.75	0	0.00	Note 1	0	Infinite	A	Web of floorbeam FB78
Angle	3.25	0	0.00	Note 1	0	Infinite	A	Angle of floorbeam FB78
CH_1 (FB. 77)	16.25	0	0.00	9.6	156	Infinite	A	Around the cutout of floorbeam FB77
CH_2 (FB. 77)	18.25	0	0.00	9.8	409	Infinite	A	Around the cutout of floorbeam FB77

Notes:

1. Details with S_{rmax} less than the stress truncation level used for the fatigue calculations are assigned 0 cycles/day and S_{reff} can not be calculated.
2. Remaining life assumes time equal to zero starts in 2004 where original base material was removed during retrofit since previous fatigue damaged areas have been removed.

Table 6.3 - Summary of fatigue life calculations of CH_1, CH_2, and CH_17 through CH_20 installed at the lateral shelf plate detail

7.0 Summary and Conclusions

Two prototype retrofits were investigated at the connections of floorbeam FB77 and floorbeam FB78. Field testing of the initial retrofit at FB77 was conducted to characterize the response of the floorbeam to moving loads of known weight. High stress-range cycles were recorded by some of the monitored channels. The maximum measured stress range was 27.5 ksi recorded by CH_2 in the crawl test CRL_TEST adjacent to the cutout. In addition to controlled load testing, remote monitoring of the floorbeam was conducted for a period of 11 days. Stress-range histograms were generated for the monitored channels and revealed that although future fatigue cracking would not be expected to control, higher than desired stresses were produced.

The stress range experienced by the details in floorbeam FB77 was slightly reduced after the removal of eighteen of the rivets used in the shear connection between the floorbeam web and the truss hanger. The retrofitted floorbeam with the rivets removed was monitored for 6.75 days. Although removing the rivets was slightly, effective in reducing the magnitude of the stresses on the web around the cutout near the connection angle.

A second retrofit was proposed by the firm of URS and implemented at floorbeam FB78 in order to further reduce stress ranges. Remote monitoring of the prototype retrofit was conducted for a period of 1.4 days. The data collected over the monitored period showed a substantial reduction in the magnitude of stresses in the web adjacent to the cutout. The second retrofit was capable of reducing the maximum measured stresses by approximately 50% at the critical locations and resulted in calculated fatigue lives that were infinite at all locations monitored.

References

1. URS Corporation, “Girard Point Bridge: TS&L/Bridge Rehabilitation Report”

Appendix A

Instrumentation Plans

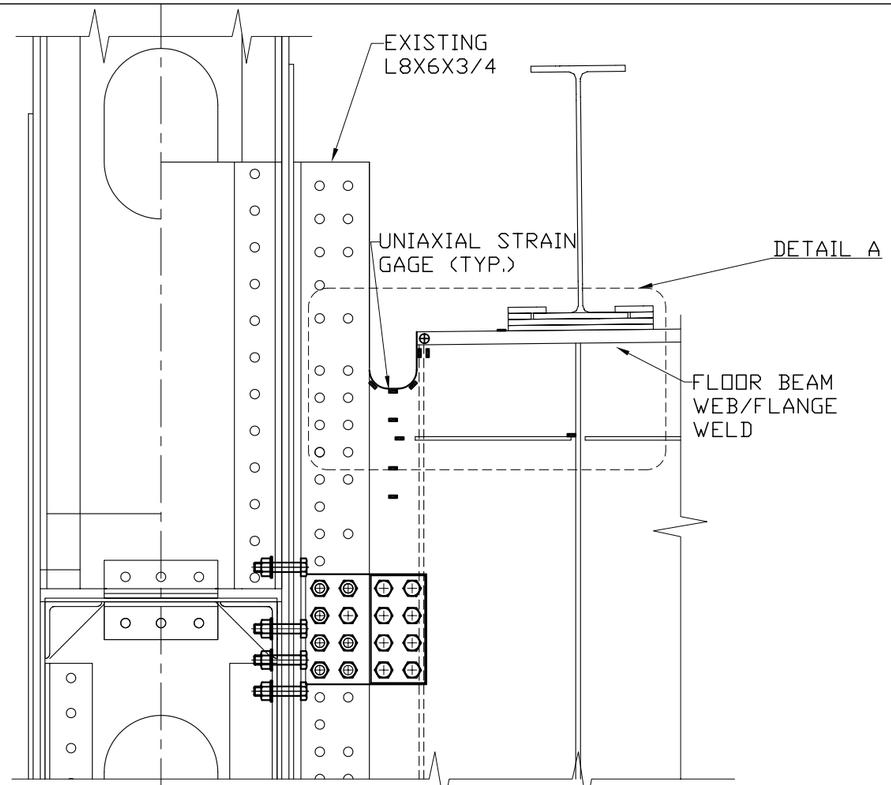

ELEVATION VIEW: FLOORBEAM/TRUSS CONNECTION (FB77)
SCALE: 3/4"=1'-0"

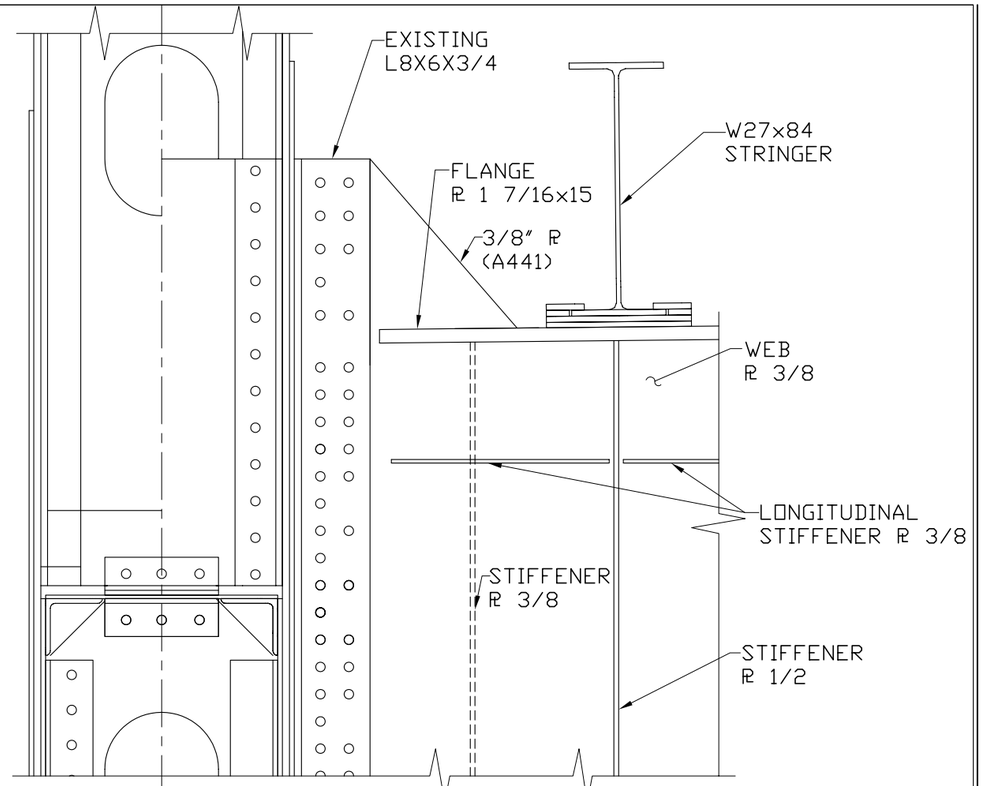

ELEVATION VIEW: EXISTING FLOORBEAM/TRUSS CONNECTION (FB77)
SCALE: 3/4"=1'-0"

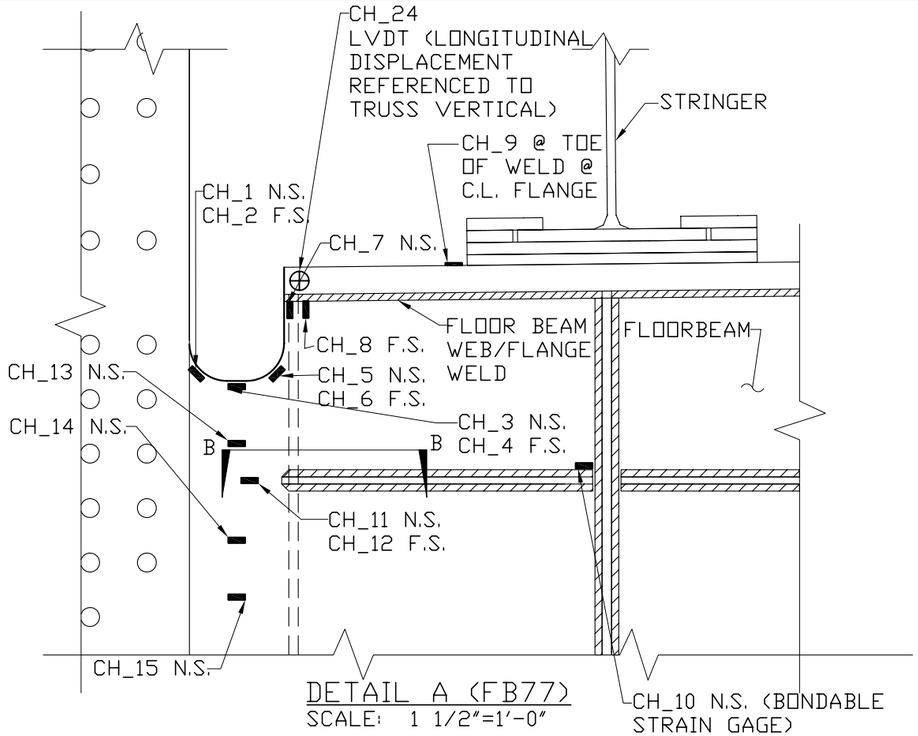

DETAIL A (FB77)
SCALE: 1 1/2"=1'-0"

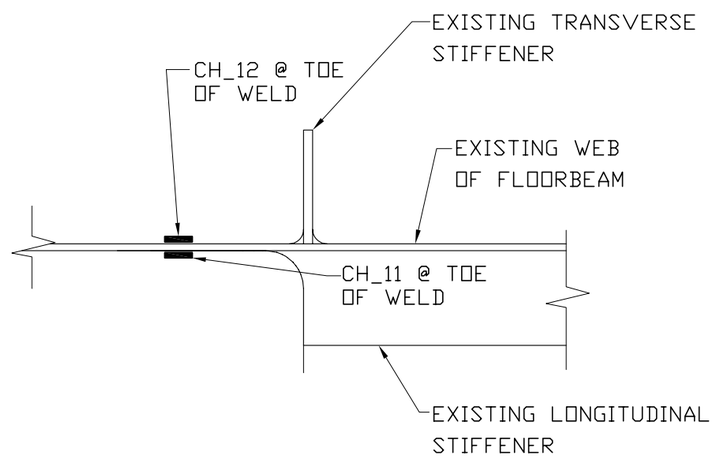

SECTION B-B (FB77)
SCALE: 6"=1'-0"

ATLSS
ADVANCED TECHNOLOGY FOR
LARGE STRUCTURAL SYSTEMS
117 ATLSS Drive
Lehigh University
Bethlehem, PA 18015
610-758-3535 FAX 610-758-6842

PROJECT:

GIRARD POINT BRIDGE SR-0095 PHILADEPHIA, PA

SHEET NOTES:

1. ALL STRAIN GAGES TO BE MEASUREMENTS GROUP, INC. WELDABLE RESISTANCE GAGES TYPE LWK-06-W2508-350, UNLESS OTHERWISE NOTED.
2. FOUR (4) ADDITIONAL STRAIN GAGES ARE TO BE INSTALLED ON THE TRUSS AND STRINGERS. EXACT LOCATIONS ARE T.B.D. IN FIELD.

NO.	DESCRIPTION	DATE	BY

DESIGNED BY:	RJC/ICH/HUM
DRAWN BY:	SEM
CHECKED BY:	HUM
SCALE:	AS SHOWN
DATE:	9/22/04
PROJECT NO.:	AT139.2
SHEET TITLE:	

INSTRUMENTATION PLAN

SHEET NO.:

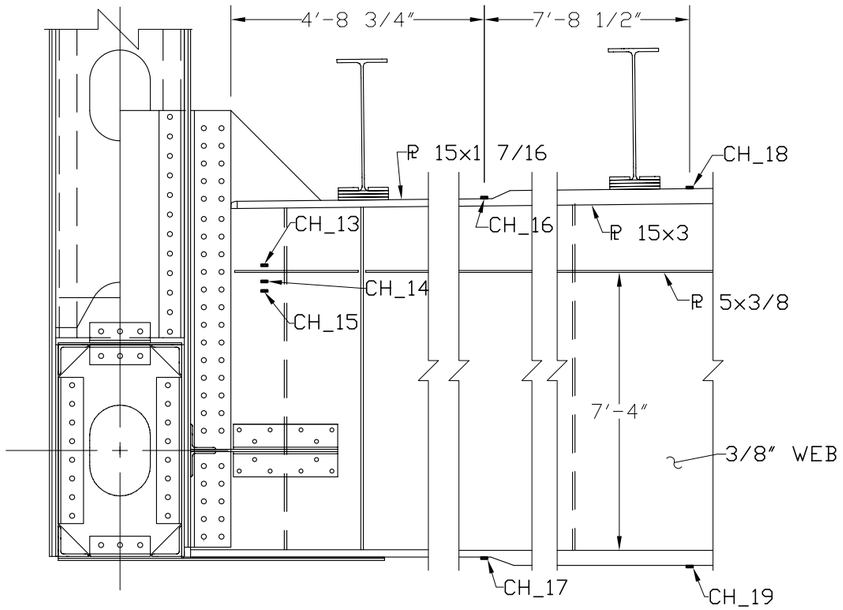

ELEVATION VIEW: FLOORBEAM (FB77)
SCALE: 1/4″=1′-0″

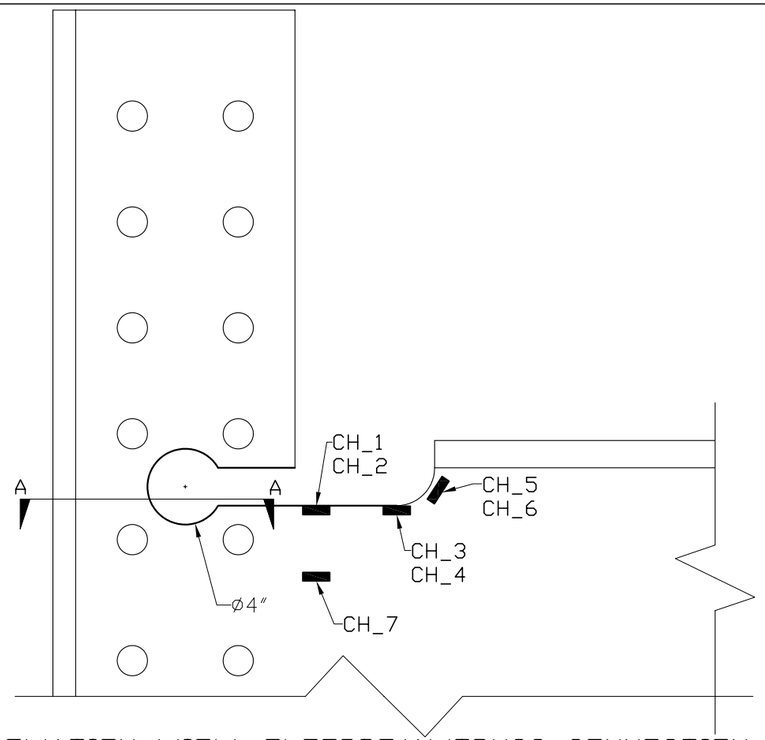

ELEVATION VIEW: FLOORBEAM/TRUSS CONNECTION (FB78)
SCALE: 1 1/2″=1′-0″

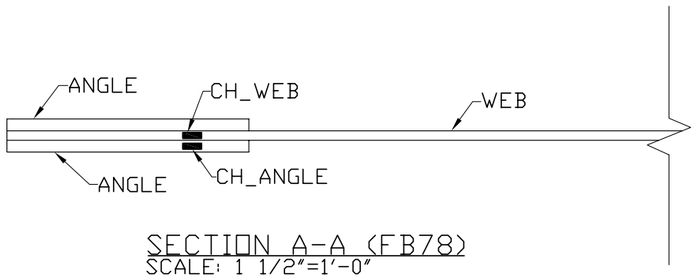

SECTION A-A (FB78)
SCALE: 1 1/2″=1′-0″

ATLSS
ADVANCED TECHNOLOGY FOR LARGE STRUCTURAL SYSTEMS
117 ATLSS Drive
Lehigh University
Bethlehem, PA 18015
610-758-3535 FAX 610-758-6842

PROJECT:

GIRARD POINT BRIDGE SR-0095 PHILADEPHIA, PA

SHEET NOTES:

1. ALL STRAIN GAGES TO BE MEASUREMENTS GROUP, INC. WELDABLE RESISTANCE GAGES TYPE LWK-06-W2508-350, UNLESS OTHERWISE NOTED.
2. FOUR (4) ADDITIONAL STRAIN GAGES ARE TO BE INSTALLED ON THE TRUSS AND STRINGERS. EXACT LOCATIONS ARE T.B.D. IN FIELD.

NO.	DESCRIPTION	DATE	BY

DESIGNED BY:	RJC/ICH/HUM
DRAWN BY:	SEM
CHECKED BY:	HUM
SCALE:	AS SHOWN
DATE:	9/22/04
PROJECT NO.:	AT139.2

SHEET TITLE:

INSTRUMENTATION PLAN

SHEET NO.: